HCV minigenome may require authentic 5′ and 3′ ends without overhang, the cassette was juxtaposed precisely at the T7 transcription start site and was followed by self-cleaving HDV ribozyme (36). Huh-NNRZ cells, a Huh-7-derived cell line stably replicating the HCV subgenomic replicon (22, 25, 42), were transfected with each reporter vector, pAM8-1 plasmid expressing T7 RNA polymerase (40) and pGL3-Control vector. The cell lysates were collected and *Renilla* luciferase activities were measured 48 h after transfection. The firefly luciferase (Fluc) activity from cotransfected pGL3-Control vector was simultaneously measured to normalize the transfection efficiency. As shown in Fig. 1B, the expression of *Renilla* luciferase, which directly reflects the level of minus-strand RNA synthesized, was only detected in cells transfected with pT7cRLNS5B1, which contains the NS5B coding region from nucleotides 9067 to 9371 upstream of 3′ UTR. Neither of the cells transfected with pT7cRLNS5B2 and pT7cRLUTR, which respectively contain the NS5B coding region from nucleotides 9307 to 9371 plus 3′-UTR and 3′-UTR alone, expressed *Renilla* luciferase. This indicates that the 3′ part of NS5B coding region from nucleotides 9067 to 9306 contains one or more *cis*-acting elements, which are absolutely required for HCV minus-strand RNA synthesis. Importantly, the *Renilla* luciferase activity in Huh-NNRZ cells transfected with pT7cRLNS5B1 alone (not cotransfection with pAM8-1) was almost negligible, providing a evidence that minus-strand RNA detected here does not result from cryptic transcription but from a HCV-dependent trans replication using minigenome transcript as a template (see below). On the basis of this finding, pT7cRLNS5B1 was used for subsequent experiments. For comparison, reporter assay with pT7RLNS5B1, pT7RLNS5B2 and pT7RLUTR, which different from their counterpart in that the *Renilla* luciferase gene was inserted in the opposite direction (Fig. 1A right), was also conducted. Interestingly, inclusion of the same NS5B coding sequence (9067 ~ 9306) dramatically inhibited the HCV IRES-directed *Renilla* luciferase expression in pT7RLNS5B1, suggesting that the 3′-partial NS5B coding region may contain bifunctional element(s) participating in both repression of HCV IRES-dependent translation and initiation of minus-strand RNA synthesis to coordinate these two processes.

To further rule out the possibility that the minus-strand RNAs which function as mRNAs for *Renilla* luciferase expression were transcription products by a cryptic promoter element in the 3′ part of NS5B coding region, we monitored the *Renilla* luciferase activity after transfection with RNAs in vitro transcribed from pT7cRLNS5B1. As a control, transcripts in vitro transcribed from pT7EMCVRLNS5B1, which is identical to pT7cRLNS5B1 except for the sense (not antisense) sequence of EMCV IRES and *Renilla* luciferase gene inserted between 5′- and 3′-end sequences of HCV, was also included. Capped firefly luciferase RNA was cotransfected as an internal control to normalize the transfection efficiency. As shown in Fig. 1C, *Renilla* luciferase activity was also detected in Huh-NNRZ cells transfected with cRLNS5B1 RNA, which was significantly higher than that in transfected Huh-7 cells. In contrast, after transfection with EMCVRLNS5B1 RNA, both Huh-NNRZ and Huh-7 cells expressed comparable *Renilla* luciferase, indicating that the higher level of *Renilla* luciferase expression in Huh-NNRZ cells was not due to the differences in mRNA stability and/or translation between Huh-NNRZ and Huh-7 cells. In view of this result together with the observation that the *Renilla* luciferase activity in pT7cRLNS5B1-transfected Huh-NNRZ cells was almost negligible in the absence of T7 RNA polymerase (Fig. 1B), we conclude that the minus-strand RNA was synthesized by HCV-dependent trans replication rather than transcription by a cryptic promoter element in pT7cRLNS5B1.

Specific gene expression in HCV replicon cell line. Our targeting strategy in this study is devised by inserting the antisense sequence of transgene and EMCV IRES between 5′- and 3′-end of HCV cDNA, and thus in principle, the foreign gene should be specifically expressed in HCV-infected cells containing functional replication apparatus. To verify this, the reporter vector pT7cRLNS5B1 and pAM8-1 were transfected into Huh-NNRZ, Huh-7, HepG2, 293 and A549 cells, and *Renilla* luciferase activities in the lysates were determined as described above. Figure 2A shows the only cell line with significant *Renilla* luciferase activity was Huh-NNRZ. Other cell lines, including both hepatic- and nonhepatic cells, expressed only low or undetectable levels of *Renilla* luciferase.

To further confirm that the transgene expression in pT7cRLNS5B1 is HCV-responsive, we performed strand-specific RT-PCR for minus-strand sequence using the RNA extracted from the transfectants described above. Three different controls (no RNA, no reverse transcriptase, and no primer in the reverse transcription) were included as specificity control and were negative. No minus-strand RNA was detected in the RT-PCR using 1 pg of in vitro transcribed plus-strand control RNA, confirming the strand specificity of the RT-PCR assay (Fig. 2B lane 3). Fully consistent with the results from reporter assay, minus-strand RNA was only detected in Huh-NNRZ cells cotransfected with pT7cRLNS5B1 and pAM8-1, while other transfected cells were negative. Simultaneously, the extracted RNA was subjected to Northern blot analysis using digoxigenin-labeled sense and antisense *Renilla* luciferase probes to detect plus- and minus-strand transcripts. Similar to the result from strand-specific RT-PCR, minus-strand RNA transcripts of the expected size (2.46 kb in length) were specifically detected in Huh-NNRZ cells transfected with pT7cRLNS5B1 and pAM8-1, although the plus-strand transcripts detected were comparable among different cell lines

FIG. 2. Specific gene expression in HCV replicon cell line. (A) The indicated cell lines were cotransfected with the pT7cRLNS5B1 and pAM8-1 vectors. Relative *Renilla* luciferase activities in the lysates were determined as described for Fig. 1. The columns and bars represent the means and standard deviations of two separate triplicate experiments. (B) Total RNAs were prepared from each transfectant. Strand-specific RT-PCR for minus-strand RNA was performed using 1 μg of extracted RNA. The arrow indicates the expected 408-bp PCR products. (C) Northern blot was performed on 5 μg of extracted RNA using digoxigenin-labeled sense and antisense *Renilla* luciferase RNA probes to detect plus- (upper panel) and minus-strand (middle panel) transcripts. Glyceraldehyde-3-phosphate dehydrogenase (GAPDH) served as a loading control. RNA size markers are shown on the left, and the bands corresponding to plus- and minus-strand RNA are indicated on the right.

(A)

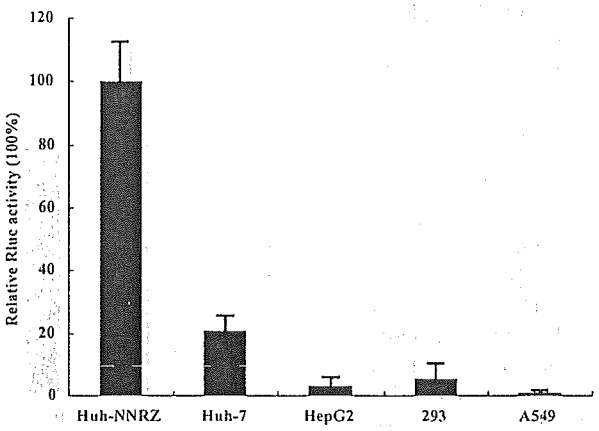
Relative Rluc activity (100%)
120
100
80
60
40
20
0
Huh-NNRZ
Huh-7
HepG2
293
A549

(B)

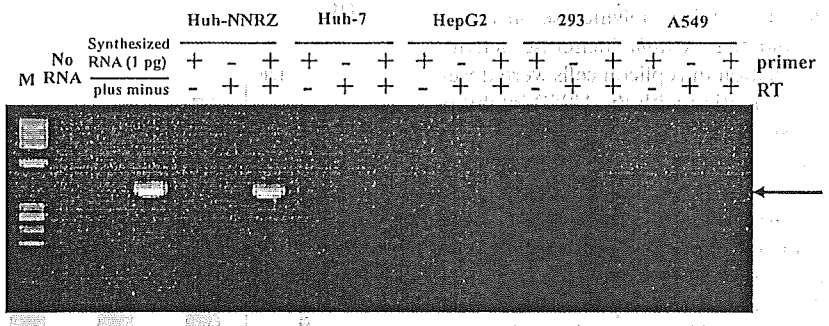
Huh-NNRZ
Huh-7
HepG2
293
A549
Synthesized RNA (1 pg)
No RNA
M
plus minus
primer
RT

(C)

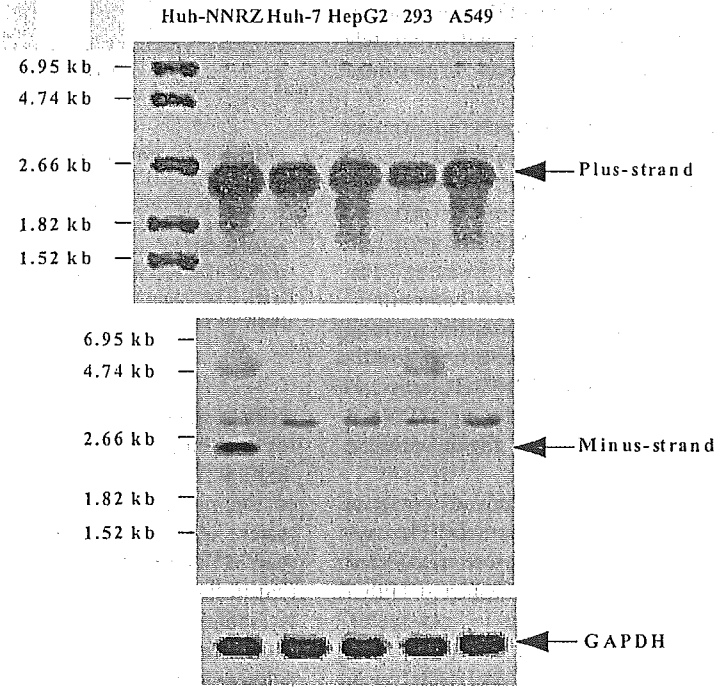
Huh-NNRZ Huh-7 HepG2 293 A549
6.95 kb
4.74 kb
2.66 kb
1.82 kb
1.52 kb
Plus-strand
Minus-strand
GAPDH

(Fig. 2C). Taken together, these experiments demonstrate that our approach can selectively direct gene expression in HCV replicon cells containing functional replication components.

Inhibition of transgene expression by short interfering RNA directed against HCV NS5B. To determine if the transgene expression in pT7cRLNS5B1 was dependent on HCV replicase in the replicon cell, Huh-NNRZ cells were infected with AdsiNS5B at MOIs of 80, 30, and 10 and then cotransfected with pT7cRLNS5B1 and pAM8-1. The cell lysates were assayed for *Renilla* luciferase expression and total RNAs were subjected to real-time RT-PCR for quantification of HCV replicon RNA levels. As shown in Fig. 3, transduction with AdsiNS5B resulted in a substantial and dose-dependent reduction in the replicon RNA level, whereas the HCV RNA level in cells transduced with irrelevant AdsiGFP, expressing short interfering RNA against green fluorescent protein, even at an MOI of 80, was comparable to that in mock-infected cells. More importantly, *Renilla* luciferase expression in AdsiNS5B-transduced Huh-NNRZ cells was also dose-dependently inhibited, fully parallel to the HCV RNA levels quantified. Likewise, in an experiment investigating the effect of a nonnucleoside inhibitor of the HCV NS5B polymerase on transgene expression, it was found that *Renilla* luciferase activity and minus-strand RNA production in replicon cells were dose-dependently reduced after incubation with the NS5B inhibitor (data not shown). These observations provide further support that the transgene expression is strictly dependent on the presence of HCV replicase.

HCV-dependent gene expression from polymerase II-derived transcripts. Application of our targeting strategy to gene therapy would require expression from polymerase II RNA polymerase rather than T7-directed transcription. It has been reported for other positive-strand RNA viruses that full-length transcripts produced in the nucleus by polymerase II are delivered in a functional form into the cytoplasm (1, 20). Artificially synthesized RNA transcripts from the cDNA of positive-strand RNA viruses require that both 5′ and 3′ ends accurately reflect those found in the viral genome in order to maximize infectivity (14).

To ensure that the polymerase II-derived transcripts contain a minimal or no overhang at the 5′ end, we adapted two distinct approaches: one by positioning the viral cDNA immediately adjacent to the transcription start site of the cytomegalovirus (CMV) promoter (Fig. 4A, pmCMVcRLmpA and pmCMVcRLHD), and another by inserting a *cis*-acting hammerhead ribozyme (17) that cleaves to produce authentic 5′ end (pCMVHHcRLmpA). Similarly, to minimize the overhang at the 3′ end of polymerase II-derived transcripts, we used a synthetic, minimal poly(A) signal (37) (pmCMVcRLmpA and pCMVHHcRLmpA) or inserted the self-cleaving HDV ribozyme upstream of the unmodified bovine growth hormone poly(A) signal (pmCMVcRLHD).

To ascertain whether the polymerase II-derived transcript could act as a functional template for minus-strand RNA synthesis, Huh-NNRZ, Huh-7 and HepG2 cells were transfected with these constructs. Compared with the transfected Huh-7 or HepG2 cells, *Renilla* luciferase activities in transfected Huh-NNRZ cells were consistently higher, the order being pmCMVcRLmpA > pmCMVcRLHD > pCMVHHcRLmpA (Fig. 4B). This indicates that the polymerase II-derived transcripts, especially that from pmCMVcRLmpA, were competent as templates for minus-strand RNA synthesis, suggesting that 5′ cap structure may not impair the template ability of the polymerase II-derived transcript to replicate. The lower *Renilla* luciferase activity in cells transfected with pmCMVcRLHD or pCMVHHRZcRLmpA compared with that in the pmCMVcRLmpA transfectant may be attributable to inefficient cleavage by the ribozyme.

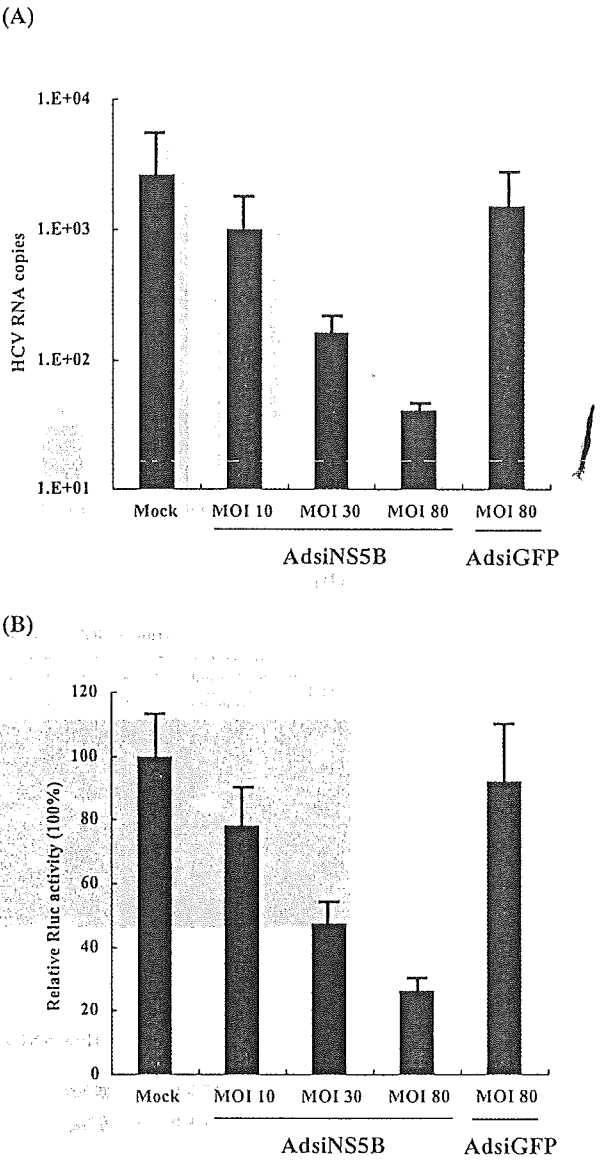

FIG. 3. Inhibition of transgene expression by silencing of HCV NS5B. Huh-NNRZ cells were infected with AdsiNS5B at an MOI of 80, 30, and 10 and then transfected with pT7cRLNS5B1 and pAM8-1. The transduced cells were harvested at day 2 posttransfection. HCV replicon RNAs were quantified with real-time RT-PCR (A), and relative *Renilla* luciferase activities were determined as described for Fig. 1 (B). The columns and bars represent the means and standard deviations of two independent experiments.

Chemosensitizing effect of CD expressed from adenovirus-delivered HCV-like minigenome. To further investigate the therapeutic feasibility of our targeting approach, we next sub-

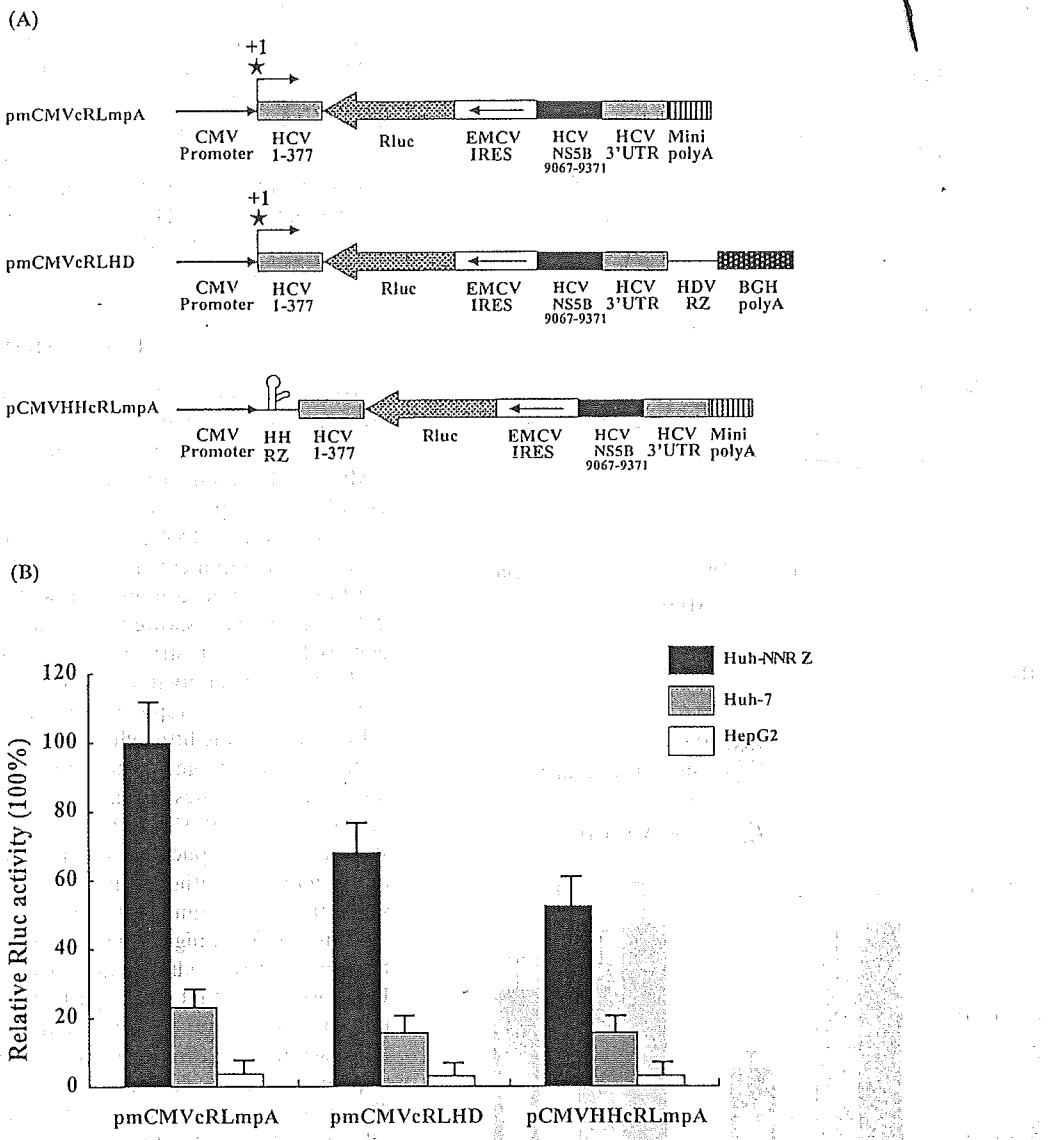

FIG. 4. Polymerase II-derived transcripts are functional templates for minus-strand RNA synthesis. (A) Schematic diagram of polymerase II-directed HCV minigenome reporter constructs. The HCV minigenome containing the antisense sequence of *Renilla* luciferase and the EMCV IRES flanked by the 5′ end (1 to 377) and 3′ partial NS5B coding region (9067 to 9371)-connected 3′ UTR was placed immediately next to the cytomegalovirus transcription start site or combined with a hammerhead ribozyme and was followed by a minimal poly(A) or HDV ribozyme upstream of the unmodified bovine growth hormone poly(A). (B) Huh-NNRZ, Huh-7, and HepG2 cells were transfected with the indicated reporter vectors. Relative *Renilla* luciferase activities in the lysates were determined as described for Fig. 1. The columns and bars represent the means and standard deviations of two separate triplicate transfections.

cloned the expression cassette from pmCMVcCDmpA, which contains the antisense sequence of the CD suicide gene instead of the *Renilla* luciferase in pmCMVcRLmpA, into recombinant adenovirus to generate AdmCMVcCDmpA. CD is a prokaryotic enzyme capable of converting the nontoxic prodrug 5-FC to the chemotherapeutic agent 5-fluorouracil (5-FU), which has been widely used in anticancer gene therapy (9, 16). Huh-NNRZ and Huh-7 cells were infected with AdmCMVcCDmpA at an MOI of 0, 10, 20, 50, 100, and 200. After 48 h, cells were harvested and CD enzymatic activity was determined by measuring the conversion of 5-FC to 5-FU. There was a dose-dependent increase in CD activity in Huh-NNRZ cells infected with AdmCMVcCDmpA, while infected Huh-7 cells showed only basal levels of CD activity, demonstrating an HCV-specific CD expression from AdmCMVcCDmpA (Fig. 5A).

To further verify the data from the enzymatic assay, we next investigated whether Huh-NNRZ cells are sensitized to the cytotoxic effect of 5-FC by transduction of AdmCMVcCDmpA. Huh-NNRZ and Huh-7 cells were infected with AdmCMVcCDmpA at an MOI of 80, followed by the addition of 5-FC (0.5 mM). Controls included AdmCMVcCDmpA alone, 5-FC alone, and no treatment. Four days later, the cytotoxic effects were evaluated with cell proliferation reagent WST-1.

Following a 4-day exposure to 5-FC, the viable cell count

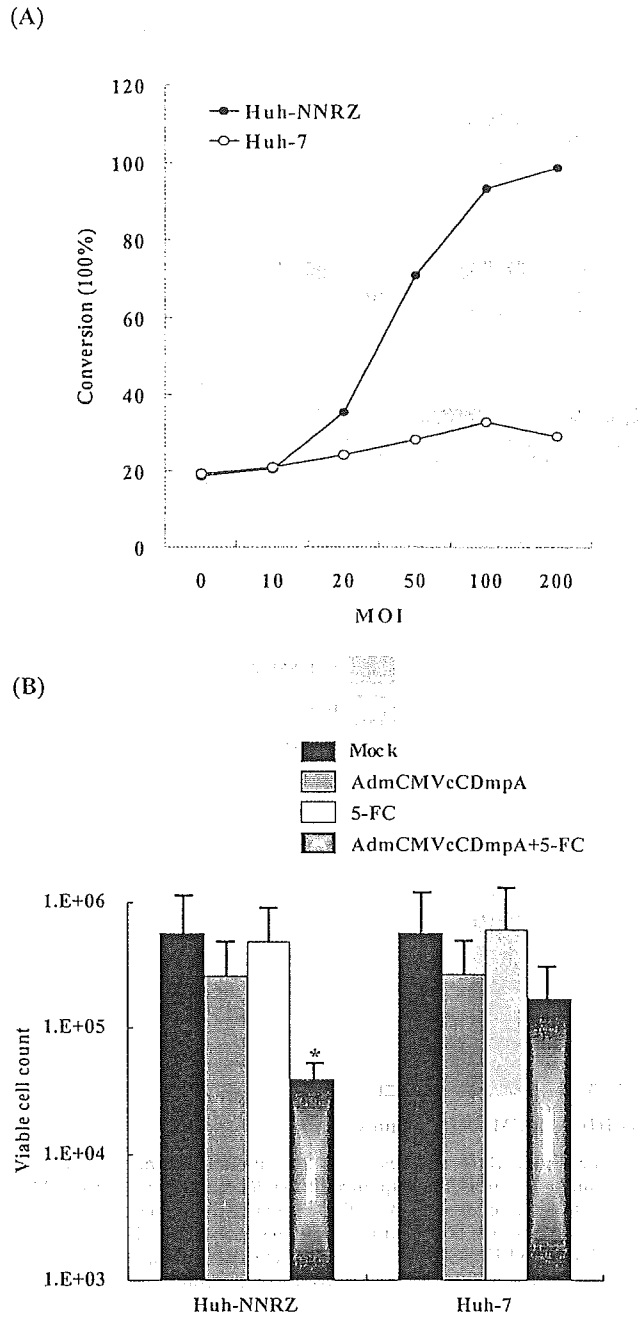

FIG. 5. Adenovirus-delivered HCV-responsive CD expression. (A) Huh-NNRZ and Huh-7 cells were infected with AdmCMVcCDmpA (MOI, 0 to 200). After 48 h, cells were harvested and CD enzymatic activity was determined by measuring the conversion of 5-FC to 5-FU. (B) Huh-NNRZ and Huh-7 cells were mock infected or infected with AdmCMVcCDmpA at an MOI of 80 and maintained in the absence or presence of 5-FC. Viable cells were quantified after 4 days. Representative data are from three separate experiments. *, $P < 0.05$ compared with the control.

of Huh-NNRZ cells transduced with AdmCMVcCDmpA was reduced by 14-fold (compared to the control, $P < 0.05$), whereas the viability of Huh-NNRZ cells infected with AdmCMVcCDmpA in the absence of 5-FC or treated with 5-FC alone was comparable to that of the control with no treatment (Fig. 5B). In contrast, transduction with AdmCMVcCDmpA did not significantly confer sensitivity to 5-FC on parental Huh-7 cells, indicating that the deaminating reaction converting 5-FC to 5-FU did not occur in uninfected Huh-7 cells due to lack of CD expression. These results further demonstrate that our strategy, by exploiting *cis*-acting replication elements, renders transgene (CD) expression responsive to the presence of HCV, thereby approaching the goal of selectively killing HCV-infected cells in combination with 5-FC while keeping uninfected cells unharmed.

DISCUSSION

We demonstrate here a proof-of-concept for a new targeting strategy to direct gene expression responsive to HCV by using a construct containing the antisense sequence of transgene and EMCV IRES flanked by the 5′- and 3′-end regions of viral cDNA. Thus, expression of the transgene is initiated only when the minus-strand RNA has been synthesized by the functional replication components present in HCV-infected cells. By using this strategy in combination with recombinant adenovirus delivery, our data showed that expression of the therapeutic gene (CD) depends strictly on the presence of functional HCV replication machinery in replicon cell, resulting in marked chemosensitization of replicon cells to the cytotoxic effects of 5-FC, while having little effect on noninfected cells. In addition to the CD suicide gene, other therapeutic genes such as apoptosis-inducing genes may also be employed in this strategy for eradication of HCV-infected cells. These experiments also show that viral replication components, including RdRp, can act in *trans* to synthesize minus-strand RNA using the transcript from the engineered construct as a template.

Using HCV minigenome reporter vectors with differently truncated NS5B coding sequences fused upstream of the 3′ UTR, we found that the 3′ part of NS5B coding region from nucleotides 9067 to 9371 is required for HCV minus-strand RNA synthesis, although it is not excluded that this *cis*-acting sequence could be further reduced by deletion mutagenesis. This result is in agreement with that reported by You et al. (39), who identified a stem-loop (5BSL3.2) at nucleotides 9262 to 9311 and found that both the structure and primary sequence of 5BSL3.2 are essential for HCV RNA replication. Although expression of the transgene from our engineered construct was dependent on the presence of functional HCV replication machinery in replicon cell, an over background level of *Renilla* luciferase activity was consistently observed in naïve Huh-7 cells, which was higher than in other hepatic and nonhepatic control cells (Fig. 2A). The reason for this "leaky" expression in naïve Huh-7 cells is currently unknown; one possible interpretation is antisense transcription mediated by the T7 polymerase. Further clarification of this HCV-independent expression in naïve Huh-7 cells is under way to determine whether it truly limits the possibility of using cytotoxic gene to selectively kill HCV-infected cells. If this is the case, other "mild" therapeutic genes such as interferons may be alternatively employed in this targeting strategy; directing HCV-responsive interferon expression should be advantageous to avoid toxic side effects.

While a low but detectable *Renilla* luciferase activity was observed, *Renilla* luciferase RNA was not detected in Huh-7

cells by Northern blot analysis (Fig. 2C). This discordance may be attributable to a lower sensitivity of the Northern blot compared to the luciferase assay. Similarly, because using RT-PCR for detection of minus-strand RNA is likely to create false positive due to self-priming or random priming of the wrong strand during the RT step, a compromise between sensitivity and strand specificity is required despite efforts to reduce such nonspecific cDNA synthesis. For this reason, to ensure high strand specificity, the sensitivity of the strand-specific RT-PCR procedure used here was limited, which may account for the failure to detect low-level *Renilla* luciferase coding transcripts in Huh-7 cells. Further experimentation is in progress to elucidate whether the discrepancy in the results of the reporter assay and Northern blot or strand-specific RT-PCR is simply due to the variance in the sensitivity of different assays.

Consistent with those reported previously (27), our study demonstrated that polymerase II-derived transcripts are competent as templates for minus-strand RNA synthesis by the HCV replication complex. Compared with the T7 expression system, polymerase II expressed lower levels of the *Renilla* luciferase reporter gene, probably due to the lower levels of polymerase II-derived transcript present in transfected cells. Additionally, while rapid amplification of cDNA end analysis of the transcript from pmCMVcRLmpA, which was constructed by trial and error to position the 5′ UTR 4 nucleotides downstream from the putative start site, confirmed that the transcription start site coincided with the first nucleotide of the 5′ UTR, it was shown that this RNA transcript terminated 14 nucleotides downstream of the AAUAA poly(A) signal. Thus, the transcript from pmCMVcRLmpA still contained an overhang of 32 nucleotides at the 3′ end, although it was much shortened by using a minimal poly(A) signal. Further efforts to minimize the overhang at the 3′ end of the polymerase II-derived transcript may be necessary to improve its template activity for minus-strand synthesis.

In an experiment to investigate the duration of reporter gene (*Renilla* luciferase) expression using pT7cRLNS5B1 (data not shown), we found that *Renilla* luciferase activity decreased considerably at day 4 and was insignificant at day 6 posttransfection, suggesting that the newly synthesized minus-strand RNA may be incompetent as a template for subsequent plus-strand production. The reason for this is currently unknown, but one possibility is that plus-strand RNA synthesis may require another *cis*-acting element(s) in addition to those included in our construct. Studies are under way to define this, as well as to identify the minimal *trans*-acting viral components essential for HCV replication, which will shed light on the development of HCV element-based gene delivery system.

Synthetic minigenomes have been described in a number of minus-stranded RNA viruses of several different families (28, 32) and plus-stranded RNA viruses belonging to the *Coronaviridae* family (19). Coupled with infectious helper viruses or plasmid-encoded proteins, minigenomes have contributed greatly to the analysis of *cis*-acting sequences and *trans*-acting proteins required for viral replication, maturation, and packaging. In addition, coronavirus-derived minigenomes have been used to express transgene in tissue culture and in animals (2). Different from the coronavirus minigenomes with the transgene in the sense orientation, which directs tissue-specific transgene expression by virtue of viral tropism, the HCV minigenome described here contains the transgene and IRES element in the antisense orientation, and the minus-strand RNA synthesized by the replication machinery in HCV-infected cells functions as the mRNA for transgene expression, rendering transgene expression responsive to the presence of HCV. However, when the antisense sequence of the reporter gene was inserted in the minigenome derived from transmissible gastroenteritis virus, the transgene was not expressed (19). Whether the discrepancy between the finding in transmissible gastroenteritis virus and that presented here is simply due to the lack of the IRES element for translation initiation in the former minigenome or due to the intrinsic difference between transmissible gastroenteritis virus and HCV remains to be investigated.

Because the HCV genome RNA and the therapeutic minigenome share the same replication machinery in infected cells, it is possible that replication of the HCV genome may be competitively inhibited when the replication machinery is being actively recruited by the therapeutic HCV minigenome. If this is the case, an additive antiviral effect may be expected. Additionally, given that the HCV-responsive expression construct described here contains the 5′ (nucleotides 1 to 377) region of the HCV genome, which was reported to interact with HCV nucleocapsid (core) protein and play an important role in viral encapsidation (11, 33, 35, 41), it is tempting to speculate that the HCV minigenome may also be packaged inside the virion and budded from infected cells and, if so, it could direct secondary transgene expression by sequential infection, ultimately augmenting its anti-HCV effect.

In summary, we have developed a novel targeting therapeutic approach directed against cells containing the HCV replication apparatus, which may be useful as a prophylactic in the early stage of hepatitis, during limited infection of the liver, or for ex vivo therapy of hepatocytes. It may also reduce virus loads in chronically infected patients and, in combination with interferon and ribavirin therapy, might eradicate HCV from the infected host. In addition to its therapeutic application, the HCV minigenome reported in this study also offers a useful tool for studies aimed at investigation of the molecular mechanisms involved in replication and expression of the HCV genome.

REFERENCES

1. Almazan, F., J. M. Gonzale, Z. Penzes, A. Izeta, E. Calvo, J. Plana-Duran, and L. Enjuanes. 2000. Engineering the largest RNA virus genome as an infectious bacterial artificial chromosome. Proc. Natl. Acad. Sci. USA 97: 5516–5521.
2. Alonso, S., I. Sola, J. P. Teifke, I. Reimann, A. Izeta, M. Balasch, J. Plana-Durán, R. J. M. Moormann, and L. Enjuanes. 2002. In vitro and in vivo expression of foreign genes by transmissible gastroenteritis coronavirus-derived minigenomes. J. Gen. Virol. 83:567–579.
3. Alter, M. J., H. S. Margolis, K. Krawczynski, F. N. Judson, A. Mares, W. J. Alexander, P. Y. Hu, J. K. Miller, M. A. Gerber, R. E. Sampliner, E. L. Meeks, and M. J. Beach. 1992. The natural history of community-acquired hepatitis C virus in the United States. N. Engl. J. Med. 327:1899–1905.
4. Bartenschlager, R. 1997. Candidate targets for hepatitis C vir us-specific antiviral therapy. Intervirology. 40:378–393.
5. Behrens, S. E., L. Tomei, and R. De Francesco. 1996. Identification and properties of the RNA-dependent RNA polymerase of hepatitis C virus. EMBO J. 15:12–22.
6. Blight, K. J., A. A. Kolykhalov, K. E. Reed, E. V. Agapov, and C. M. Rice. 1998. Molecular virology of hepatitis C virus: an update with respect to potential antiviral targets. Antivir. Ther. 3:71–81.
7. Cheng, J.-C., M.-F. Chang, and S. C. Chang. 1999. Specific interaction between the hepatitis C virus NS5B RNA polymerase and the 3′ end of the viral RNA. J. Virol. 73:7044–7049.
8. Choo, Q.-L., K. H. Richman, J. H. Han, K. Berger, C. Lee, C. Dong, C.

Gallegos, D. Coit, A. Medina-Selby, P. J. Barr, A. J. Weiner, D. W. Bradley, G. Kuo, and M. Houghton. 1991. Genetic organization and diversity of the hepatitis C virus. Proc. Natl. Acad. Sci. USA 88:2451–2455.
9. Danielsen, S., M. Kilstrup, K. Barilla, B. Jochimsen, and J. Neuhard. 1992. Characterization of the *Escherichia coli codBA* operon encoding cytosine permease and cytosine deaminase. Mol. Microbiol. 6:1335–1344.
10. Dhanak, D., K. J. Duffy, V. K. Johnston, J. Lin-Goerke, M. Darcy, A. N. Shaw, B. Gu, C. Silverman, A. T. Gates, M. R. Nonnemacher, D. L. Earnshaw, D. J. Casper, A. Kaura, A. Baker, C. Greenwood, L. L. Gutshall, D. Maley, A. DelVecchio, R. Macarron, G. A. Hofmann, Z. Alnoah, H. Y. Cheng, G. Chan, S. Khandekar, R. W. Keenan, and R. T. Sarisky. 2002. Identification and biological characterization of heterocyclic inhibitors of the hepatitis C virus RNA-dependent RNA polymerase. J. Biol. Chem. 277:38322–38327.
11. Fan, Z., Q. R. Yang, J. S. Twu, and A. H. Sherker. 1999. Specific in vitro association between the hepatitis C viral genome and core protein. J. Med. Virol. 59:131–134.
12. Friebe, P., and R. Bartenschlager. 2002. Genetic analysis of sequences in the 3′ untranslated region of hepatitis C virus that are important for RNA replication. J. Virol. 76:5326–5338.
13. Grakoui, A., D. W. McCourt, C. Wychowski, S. M. Feinstone, and C. M. Rice. 1993. Characterization of the hepatitis C virus-encoded serine proteinase: determination of proteinase-dependent polyprotein cleavage sites. J. Virol. 67:2832–2843.
14. Herold, J., and R. Andino. 2000. Poliovirus requires a precise 5′ end for efficient positive-strand RNA synthesis. J. Virol. 74:6394–6400.
15. Hijikata, M., N. Kato, Y. Ootsuyama, M. Nakagawa, and K. Shimotohno. 1991. Gene mapping of the putative structural region of the hepatitis C virus genome by in vitro processing analysis. Proc. Natl. Acad. Sci. USA 88:5547–5551.
16. Hirschowitz, E. A., A. Ohwada, W. R. Pascal, T. J. Russi, and R. G. Crystal. 1995. *In vivo* adenovirus-mediated gene transfer of the Escherichia coli cytosine deaminase gene to human colon carcinoma-derived tumors induce chemosensitivity to 5-fluorocytosine. Hum. Gene. Ther. 6:1055–1063.
17. Huang, Y., and G. C. Carmichael. 1996. Role of polyadenylation in nucleocytoplasmic transport of mRNA. Mol. Cell. Biol. 16:1534–1542.
18. Ideo, G., and A. Bellobuono. 2002. New therapies for the treatment of chronic hepatitis C. Curr. Pharm. Des. 8:959–966.
19. Izeta, A., C. Smerdou, S. Alonso, Z. Penzes, A. Mendez, J. Plana-Duran, and L. Enjuanes. 1999. Replication and packageing of transmissible gastroenteritis coronavirus-derived synthetic minigenomes. J. Virol. 73:1535–1545.
20. Khromykh, A. A., A. N. Varnavski, P. L. Sedlak, and E. G. Westaway. 2001. Coupling between replication and packaging of flavivirus RNA: Evidence derived from the use of DNA-based full-length cDNA clones of Kunjin virus. J. Virol. 75:4633–4640.
21. Kieft, J. S., K. hou, A. Grech, R. Jubin, and J. A. Doudna. 2002. Crystal structure of an RNA tertiary domain essential to HCV IRES-mediated translation initiation. Nat. Struct. Biol. 9:370–374.
22. Kishine, H., K. Sugiyama, M. Hijikata, N. Kato, H. Takahashi, T. Noshi, Y. Nio, M. Hosaka, Y. Miyanari, and K. Shimotohno. 2002. Subgenomic replicon derived from a cell line infected with the hepatitis C virus. Biochem. Biophys. Res. Commun. 293:993–999.
23. Kuriyama, S., K. Masui, T. Sakamoto, T. Nakatani, M. Kikukawa, H. Tsujinoue, A. Mitoro, M. Yamazaki, H. Yoshiji, H. Fukui, K. Ikenaka, C. A. Mullen, and T. Tsujii. 1998. Bystander effect caused by cytosine deaminase gene and 5-fluorocytosine *in vitro* is substantially mediated by generated 5-fluorouracil. Anticancer Res. 18:3399–3406.
24. Lindenbach, B. D., and C. M. Rice. 2003. Evasive maneuvers by hepatitis C virus. Hepatology 38:769–771.
25. Lohmann, V., F. Korner, J. O. Koch, U. Herian, L. Theilmann, and R. Bartenschlager. 1999. Replication of subgenomic hepatitis C virus RNAs in a hepatoma cell line. Science 285:110–113.
26. Lu, L., T. J. Pilot-Matias, K. D. Stewart, J. T. Randolph, R. Pithawalla, W. He, P. P. Huang, L. L. Klein, H. Mo, and A. Molla. 2004. Mutations conferring resistance to a potent hepatitis C virus serine protease inhibitor in vitro. Antimicrob. Agents Chemother. 48:2260–2266.
27. McCormick, C. J., L. Challinor, A. Macdonald, D. J. Rowlands, and M. Harris. 2004. Introduction of replication-competent hepatitis C virus transcripts using a tetracycline-regulable baculovirus delivery system. J. Gen. Virol. 85:429–439.
28. Mühlberger, E., M. Weik, V. Volchkov, H. –D. Klenk, and S. Becker. 1999. Comparison of the transcription and replication strategies of Marburg virus and Ebola virus by using artificial replication systems. J. Virol. 73:2333–2342.
29. Nguyen, T. T., A. T. Gates, L. L. Gutshall, V. K. Johnston, B. Gu, K. J. Duffy, and R. T. Sarisky. 2003. Resistance profile of a hepatitis C virus RNA-dependent RNA polymerase benzothiadiazine inhibitor. Antimicrob. Agents Chemother. 47:3525–3530.
30. Oh, J. W., T. Ito, and M. M. C. Lai. 1999. A recombinant hepatitis C virus RNA-dependent RNA polymerase capable of coping the full-length viral RNA. J. Virol. 73:7694–7702.
31. Oh, J. W., G. T. Sheu, and M. M. C. Lai. 2000. Template requirement and initiation site selection by hepatitis C virus polymerase on a minimal viral RNA template. J. Bio. Chem. 275:17710–17717.
32. Perez, M., A. Sanchez, B. Cubitt, D. Rosario, and J. C. de la Torre. 2003. A reverse genetics system for Borna disease virus. J. Gen. Virol. 84:3099–3104.
33. Ray, R. B., and R. Ray. 2001. Hepatitis C virus core protein: intriguing properties and functional relevance. FEMS Microbiol. Lett. 202:149–156.
34. Saito, I., A. Miyamura, H. Ohbayashi, H. Harada, T. Katayama, S. Kikuchi, Y. Watanabe, S. Koi, M. Onji, Y. Ohta, Q.-L. Choo, M. Houghton, and G. Kuo. 1990. Hepatitis C virus infection is associated with the development of hepatocellular carcinoma. Proc. Natl. Acad. Sci. USA 87:6540–6547.
35. Shimoike, T., S. Mimori, H. Tani, Y. Matsuura, and T. Miyamura. 1999. Interaction of hepatitis C virus core protein with viral sense RNA and suppression of its translation. J. Virol. 73:9718–9725.
36. Suh, Y. A., P. K. Kumar, K. Taira, and S. Nishikawa. 1993. Self-cleavage activity of the genomic HDV ribozyme in the presence of various diavalent metal ions. Nucleic Acids Res. 21:3277–3280.
37. Xia, H., Q. Mao, H. L. Paulson, and B. L. Davidson. 2002. siRNA-mediated gene silencing *in vitro* and *in vivo*. Nat. Biotechnol. 20:1006–1010.
38. Yi, M., and S. M. Lemon. 2003. 3′ nontranslated RNA signals required for replication of hepatitis C virus RNA. J. Virol. 77:3557–3568.
39. You, S., D. D. Stump, A. D. Branch, and C. M. Rice. 2004. A *cis*-acting replication element in the sequence encoding the NS5B RNA-dependent RNA polymerase is required for hepatitis C virus RNA replication. J. Virol. 78:1352–1366.
40. Zhang, J., O. Yamada, T. Ito, M. Akiyama, Y. Hashimoto, H. Yoshida, R. Makino, A. Masago, H. Uemura, and H. Araki. 1999. A single nucleotide insertion in the 5′-untranslated region of hepatitis C virus leads to enhanced cap-independent translation. Virology 261:263–270.
41. Zhang, J., O. Yamada, H. Yoshida, T. Iwai, and H. Araki. 2002. Autogenous translational inhibition of core protein: implication for switch from translation to RNA replication in hepatitis C virus. Virology 293:141–150.
42. Zhang, J., O. Yamada, K. Sakamoto, H. Yoshida, T. Iwai, Y. Matsushita, H. Shimamura, H. Araki, and K. Shimotohno. 2004. Down-regulation of viral replication by adenoviral-mediated expression of short interfering RNA against cellular cofactors for hepatitis C virus. Virology 320:135–143.

Original Paper

Intervirology

Intervirology 2005;48:104–111
DOI: 10.1159/000081736

Received: February 5, 2004
Accepted: March 10, 2004

Analysis of the 5′ End Structure of HCV Subgenomic RNA Replicated in a Huh7 Cell Line

Hitoshi Takahashi Masashi Yamaji Masahiro Hosaka Hiroe Kishine
Makoto Hijikata Kunitada Shimotohno

Institute for Virus Research, Kyoto University, Sakyo-ku, Kyoto, Japan

Key Words
Hepatitis C virus · Genome replication · 5′ end · Chronic hepatitis · De novo RNA synthesis

Abstract
Objective: Recently, HCV subgenomic RNA that replicates in vitro in a certain cell line have been elucidated. Since the 5′ end of the genome of positive strand RNA viruses is often modified with a cap structure or a covalently linked protein, we have assessed structural feature of the HCV genome obtained from Huh7 cells in which HCV subgenomic RNA has been shown to efficiently self-replicate. ***Methods:*** HCV subgenomic RNA was obtained from the Huh7 and was analyzed for its 5′ end. ***Results:*** Phosphorylation of the genomic RNA by polynucleotide kinase was observed only after treatment with phosphatase. The labeling efficiency of the genome with polynucleotide kinase was not enhanced by treatment with pyrophosphatase. ***Conclusion:*** It is suggested that the 5′ end of HCV genomic RNA obtained from HCV replicon cells is not modified except phosphorylation. Furthermore, analysis of the 5′ end of the HCV RNA obtained from the HCV subgenome self-replicating cells revealed the presence of two types of subgenomic RNA that contained either guanylate or adenylate at the 5′ end. This result indicates that the 5′ end of the subgenome in Huh7 cells is redundant and there is no significant evolutionary advantage between the two genomes.

Introduction

RNA produced from positive strand RNA viruses in eukaryotes functions as the genome, an intermediate of the genome, and mRNA during viral replication. In these viruses, the 5′ end of the genome is often capped, but there are some exceptions [1]. In the poliovirus, the 5′ end of the genomic RNA is modified by a virally encoded protein, VPg [2]. VPg functions as a primer for poliovirus-encoded RNA polymerase for the synthesis of genomic RNA and the negative strand RNA [3]. Poliovirus mRNA is generated by the cleavage of VPg from the genomic RNA and viral proteins are produced in an internal ribosome entry site (IRES)-dependent manner [4].

The hepatitis C virus (HCV) causes chronic hepatitis C and liver cirrhosis, and has been linked to the develop-

KARGER
Fax + 41 61 306 12 34
E-Mail karger@karger.ch
www.karger.com

0300–5526/05/0483–0104$22.00/0

Accessible online at:
www.karger.com/int

Kunitada Shimotohno
Institute for Virus Research, Kyoto University
Sakyo-ku
Kyoto 606-8507 (Japan)
Tel. +81 75 751 4000, Fax +81 75 751 3998, E-Mail kshimoto@virus.kyoto-u.ac.jp

ment of hepatocellular carcinoma by epidemiological research [5]. HCV is a positive strand RNA virus belonging to the Hepcvirus genus in the *Flaviviridae* family. In this family, there are two additional genera, Flavi- and Pestiviruses. Viral RNA from Flaviviruses has a capped structure and responsive enzymes such as methyltransferase and a capping enzyme are encoded in the viral non-structural (NS) 5 protein, in which RNA polymerase activity also resides [1]. This information suggests that translation of Flavivirus RNA is conducted in a cap-dependent manner. On the other hand, RNA from viruses classified into the Pestivirus and Hepcvirus genera has an IRES structure which plays an important role in cap-independent translation [6, 7].

The HCV genome consists of about 9,600 nucleotides and contains three parts: a 5′ non-coding region of 341 nucleotides containing the sequence for the IRES structure, the coding region of about 3,000 nucleotides, which encodes about 10 viral proteins, and the 3′ non-coding region of about 200 nucleotides depending on the size of the poly-uridylate track within this region [8, 9]. There is no poly-A tail at the 3′ end of the genome; instead, the 3′ end of the genome consists of uridylate [10, 11]. However, the precise structure of the 5′ end of the genome, including possible modifications, remains to be elucidated. Recent progress has established a method that enables the proliferation of the HCV genome in a cell culture system; this also makes it feasible to analyze the biological activity of the HCV genome. Using this system, several HCV sub- and full-genomic RNAs were shown to self-replicate efficiently in certain cell lines, which are known as HCV replicon cells [12]. Although some HCV RNAs synthesized in vitro have proven to be infectious in the chimpanzee, experiments with genomic HCV RNA using this animal model system are laborious [13]. In contrast, HCV replicon cells allow the analysis of the structure of the 5′ end more easily than analysis of samples obtained from liver specimens or sera from HCV-infected individuals. Taking advantage of this opportunity, we have analyzed the 5′ end structure of the HCV genome obtained from HCV replicon cells by assessing the susceptibility to phosphorylation by polynucleotide kinase before and after treatment with enzymes which are used to analyze the 5′ end structure of RNA. Moreover, we have determined the nucleotide residue at the 5′ end of the HCV genomic RNA.

Materials and Methods

Cell Line

MH-14 cells were grown in Dulbecco's modified Eagle medium supplemented with 10% fetal bovine serum, 0.1 m*M* non-essential amino acid mixture and G418.

RNA Extraction

Total RNA from MH-14 cells was extracted by Sepasol I (Nacarai Tesque, Kyoto, Japan) according to the manufacturer's protocol. Extraction of HCV subgenomic RNA was performed with an mRNA isolation kit (Roche, Tokyo) using a biotin-labeled oligonucleotide probe, 5′-biotin-TAGGATTCGTGCTCATGGTTGCACGGTCTACGAGAC-3′, which is complementary to the 5′ non-coding region of the HCV genome. The bound HCV RNA was trapped in an avidin-linked resin through the oligonucleotide and eluted from the resin by heat.

Modification of RNA by Various Enzymes

RNA was treated with 0.2 unit of bacterial alkaline phosphatase, BAP, in 0.1 *M* Tris-HCl (pH 8.0), 1 m*M* $MgSO_4$, and 40 units of RNase inhibitor (Applied Biosystems) and then subjected to a polynucleotide kinase reaction in the presence of ^{32}P-γ-ATP in 10 m*M* Tris-acetate (pH 7.6), 10 m*M* MgOAc, 50 m*M* potassium acetate, 0.185 Mbq ^{32}P-γ-ATP, and 40 units of RNase inhibitor at 37°C for 30 min. For the treatment by pyrophosphatase, RNA was incubated with 5 units of tobacco acid pyrophosphatase (TAP) in a buffer consisting of 50 m*M* sodium acetate (pH 5.0), 0.1% β-mercaptoethanol, 1 m*M* EDTA, 0.01% Triton X-100 and 40 units of RNase inhibitor at 37°C for 30 min. Following TAP treatment, the RNA was further treated with BAP and subjected to polynucleotide kinase reaction. The in vitro synthesized HCV subgenomic RNA was treated with BAP and polynucleotide kinase as described above.

Analysis of Mononucleotides by Thin-Layer Chromatography

The 5′ end labeled RNA was extracted from the agarose gel and was treated with 0.3 *N* NaOH for 24 h at 37°C to hydrolyze the RNA to mononucleotides. The digest was desalted by DEAE Sepharose column chromatography and subjected to thin-layer chromatography. The thin-layer plate was developed with the solvents consisting of isobutylic acid and 0.5 *M* ammonia water (5:3, vol/vol) in the first dimension, and with a solvent consisting of isopropanol, 12 *N* HCl and H_2O in volume ratios of 70:15:15 for the 2nd dimension. The signal was detected by autoradiography. The identity of each spot was determined by co-development of authentic mononucleotides in the chromatography.

Analysis of the 5′ End of RNA by Rapid Amplification of cDNA ENDs, RACE

RNA was treated with BAP and subjected to a polynucleotide kinase reaction. After this treatment, a 5′-CCCGUCUUCGGACAUCCAGAGGUAC-3′ RNA oligomer was ligated to the RNA. Reverse transcription followed by PCR was conducted using the following primers: 5′-CGCGGATCCCCCGTCTTCGGACATCCA-3′, which contains part of the sequence of the RNA oligomer, and 5′-CCGGAATTCACGCTTTCTGCGTGAAGACAG-3′, which is complementary to the 5′ region of the HCV genome. The RACE experiment was conducted according to the manufacturer's protocol. The amplified DNA was cloned into a TA-plasmid and sequenced.

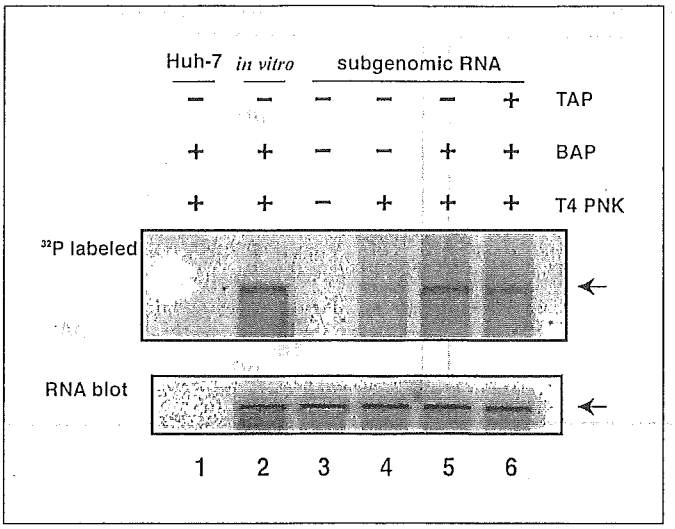

Fig. 1. Analysis of the 5′ end of HCV subgenomic RNA isolated from the HCV genome self-replicating cell line, Huh7. MH14 cells (10^7 cells), which allow the self-replication of the HCV subgenome, were harvested and total RNA was prepared using Sepasol I. The total RNA was then incubated with a biotinylated oligoDNA fragment which is complementary to the non-coding region of the HCV genome as described in Materials and Methods. The RNA was divided into three aliquots. The first RNA aliquot was treated with BAP followed by labeling of its end with a polynucleotide kinase reaction in the presence of ^{32}P-γ-ATP. The second RNA aliquot was treated with 5 units of TAP, BAP and followed by end-labeling. The third RNA aliquot was pretreated in a similar way, but without addition of any enzymes, and subjected to polynucleotide kinase reaction. The in vitro synthesized HCV subgenomic RNA was treated with BAP and polynucleotide kinase as described. Each aliquot of RNA was then divided in half and the RNAs were electrophoresed on two denaturing agarose gels in MOPS buffer. One gel was dried and analyzed by autoradiography and the other gel was subjected to Northern blot using a radio-labeled HCV RNA probe.

Results and Discussion

Analysis of the 5′ End Structure of HCV Subgenomic RNA Isolated from an HCV Replicon Cell Line, MH-14

We have previously established HCV replicon cells derived from the Huh7 cell line by transfecting HCV genomic RNA synthesized in vitro. The RNA was synthesized using information about infectious HCV RNA obtained from a human T lymphocytes line, MT-2, infected with HCV-positive plasma [14]. There were approximately a few thousand copies of HCV subgenomic RNA per replicon cell as determined by real-time reverse transcription followed by polymerase chain reaction (RT-PCR) [15, 16]. During proliferation of the HCV replicon cells, we obtained one cell clone, MH14, in which the level of HCV subgenomic RNA was 3- to 4-fold higher than in the original replicon cells [17]. The increased copy number seemed to be the result of the evolution of the HCV subgenomic RNA by nucleotide substitution as has been previously described by other groups [18]. A detailed analysis of the genome in the cell clone was reported elsewhere [19].

Total RNA from MH-14 cells was extracted by the method described in Materials and Methods. Using this method, only positive strand genomic RNA was extracted (fig. 1, data not shown). The extracted HCV RNA was divided into three aliquots. One aliquot was used without further enzymatic modification, the second aliquot was treated with bacterial alkaline phosphatase (BAP) alone, and the third aliquot was treated with tobacco acid pyrophosphatase (TAP) (Epicenter, Wisc., USA), followed by treatment with BAP. A polynucleotide kinase reaction was then carried out on all three aliquots. To generate control HCV RNA, the plasmid pNNRZ2, which carries the entire subgenome of the HCV replicon used to establish the HCV replicon cell line, was in vitro transcribed by T7 RNA polymerase. The RNA was purified by DNase I treatment followed by phenol-chloroform treatment. HCV subgenomic RNA from each preparation was semiquantitated by RT-PCR and equal amounts of HCV subgenomic RNA were radio-labeled by polynucleotide kinase reaction using ^{32}P-γ-ATP. As a control, the in vitro synthesized HCV subgenomic RNA was subjected to the polynucleotide kinase reaction in the presence of ^{32}P-γ-ATP before and after treatment with BAP. Following the polynucleotide kinase reaction, the RNA was electrophoresed in a denaturing agarose gel and subjected to autoradiography. A signal at 8 kb, the position of the intact subgenomic RNA, is expected if ^{32}P is incorporated at the 5′ end of the HCV subgenomic RNA. A very faint autoradiographic signal was detectable from the in vitro synthesized RNA subjected to the kinase reaction without BAP treatment (data not shown). In contrast, a significant incorporation of ^{32}P was observed in the sample treated with BAP prior to the polynucleotide kinase reaction (fig. 1). This result indicates that the in vitro synthesized HCV subgenomic RNA was phosphorylated at the 5′ terminus and, as expected, was resistant to the kinase reaction. Next, we conducted a kinase reaction on the HCV subgenomic RNA prepared from MH-14 cells. When the HCV RNA was subjected to the kinase reaction without BAP treatment, only a slight ^{32}P signal was detected. The level of ^{32}P incorporation increased when the kinase reaction was carried out after treatment with BAP (fig. 1,

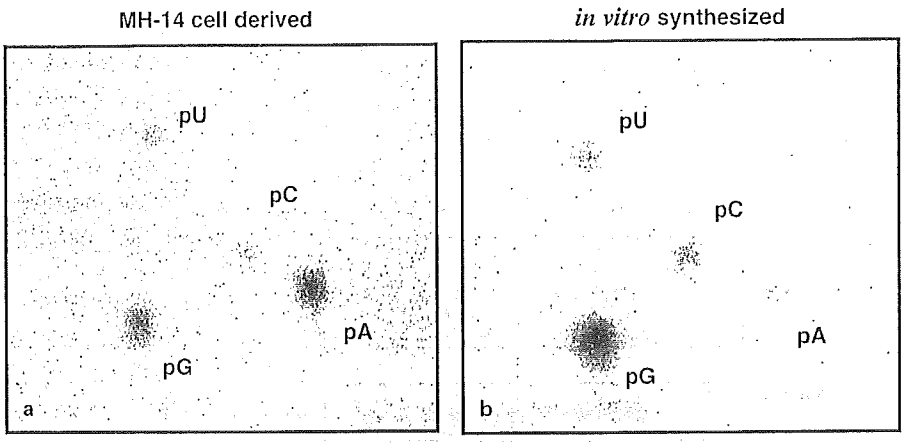

Fig. 2a, b. Analysis of nucleoside monophosphate derived from the 5′ end of the HCV subgenomic RNA. 5′ end labeled RNA as shown in figure 1, lanes 2 and 5, was extracted from the agarose gel. This RNA was treated with 0.3 *N* NaOH for 24 h at 37 °C to hydrolyze the RNA to mononucleotides. The digest was desalted by DEAE Sepharose column chromatography and subjected to thin-layer chromatography. The thin-layer plate was developed with the solvents described in the text, and the signal was detected by autoradiography. The identity of each spot was determined by co-development of authentic mononucleotide in the chromatography.

lanes 4 and 5). When HCV subgenomic RNA was treated with TAP, BAP, and then subjected to the kinase reaction, the amount of incorporation of ^{32}P was very similar to that of incorporation observed without TAP treatment (fig. 1, lanes 5 and 6). An RNA fraction obtained from Huh7 cells by the same procedure used to prepare the HCV subgenomic RNA from HCV replicon cells was used as a negative control. This RNA did not give rise to any ^{32}P signal after the kinase reaction either before or after BAP treatment (fig. 1, lane 1). To confirm that the differences in the intensity of the bands detected by autoradiography were not dependent on the amount of HCV RNA used for the analysis, the amount of RNA was analyzed by northern blot and was confirmed to be in almost the same range (fig. 1, lower panel). It is worth mentioning that the intensity of the ^{32}P signal detected in in vitro synthesized HCV RNA and the RNA obtained from Huh7 cells was almost the same (fig. 1, lanes 2 and 5). Taken together, these results indicate that the 5′ end of the majority of the HCV subgenomic RNA replicating in Huh7 cells was sensitive to BAP treatment. The fact that the phosphate residues at the end of the HCV genomic RNA were labile to BAP, and that TAP plus BAP treatment did not enhance the incorporation of ^{32}P, suggests that the 5′ end of the HCV genome does not contain a modification such as a cap or a protein linked covalently through the 5′ phosphate residue. However, the following possibilities exist: the presence of a modified structure which is resistant to pyrophosphatase treatment or the presence of a modification that does not interfere with the 5′ phosphate residue.

Whereas the poliovirus genomic RNA contains VPg, the poliovirus mRNA lacks VPg at its 5′ end, despite the fact that the nucleotide sequence of the end is the same in both genomic and messenger RNAs [20]. Considering the characteristics of poliovirus RNA polymerase, it is likely that the VPg at the end of the genomic RNA is cleaved off to generate functional mRNA. By analogy to poliovirus replication, it remains a possibility that the abundant HCV RNA in HCV replicon cells is an unmodified mRNA type, but not a genomic type. However, as described below, we think this possibility is unlikely.

Poliovirus RNA polymerase can synthesize RNA complementary to the template only in the presence of a primer RNA or in the presence of VPg in vitro [4]. However, under physiological conditions, the polymerase uses VPg as the primer exclusively. Poliovirus polymerase incorporates uridylate at the tyrosine residue of VPg and an RNA elongation reaction proceeds via addition of a nucleotide complementary to the template at the 3′ end of the uridylate residue. On the other hand, HCV NS5B does not depend on the presence of a primer for the initiation of RNA synthesis in vitro. Differences in this characteristic feature of these two enzymes also support the possibility that the HCV genome does not have a 5′ modified structure such as that of poliovirus genomic RNA.

Analysis of the Nucleotide at the 5′-Terminus of the HCV Subgenomic RNA Replicated in HCV Replicon Cells

To further analyze the structure of the 5′ end of the HCV subgenomic RNA present in the HCV replicon Huh7 cells, we radiolabeled the 5′ end with polynucleotide kinase after BAP treatment and the RNA was electrophoresed in a denaturing agarose gel as shown in figure 1. The 8-kb RNA was eluted from the gel and treated with 0.3 *N* NaOH for 24 h at 37 °C. The resulting nucleotide solution was subjected to two-dimensional thin-layer

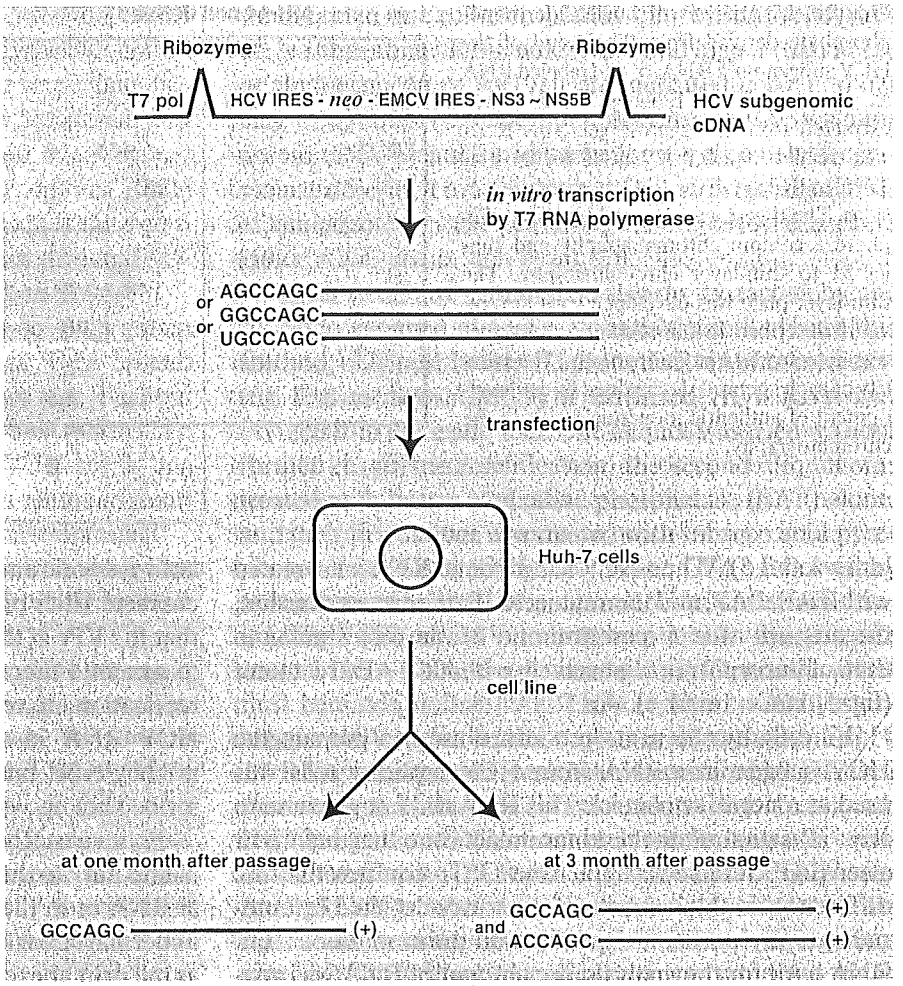

Fig. 3. A brief diagram of the HCV subgenomic RNA used to establish HCV genome replicon cells, the experimental procedure for analysis of the 5′-terminal structure, and the results of the nucleotide sequence of the 5′ end of the genome.

chromatography and developed with a solvent described in Materials and Methods. The thin layer plate was exposed to an X-ray film after development (fig. 2a). The HCV subgenomic RNA synthesized in vitro was analyzed in the same way (fig. 2b). The RNA synthesized in vitro is expected to have guanylate at the 5′ end, as determined by the structure of the pNNRZ2 plasmid. Indeed, the observed result agreed with the expectation. In addition to the major guanylate (GMP) spot, spots corresponding to uridylate (UMP), cytidylate (CMP) and adenylate (AMP) were faintly detectable. We think that the ^{32}P-UMP, ^{32}P-CMP and ^{32}P-AMP were generated by a kinase reaction acting on partially degraded HCV genomic RNA. In contrast, the RNA from the HCV replicon Huh7 cell line, MH14, gave rise to production of ^{32}P-GMP and ^{32}P-AMP as major spots, in addition to production of small amounts of ^{32}P-UMP and ^{32}P-CMP. The UMP and CMP are likely derived from RNA contaminants in the preparation of HCV genomic RNA. The same result was observed in an analysis of the 5′ end of the HCV genome prepared from other HCV replicon cells (data not shown). Sequence data shows that the first adenylate residue downstream of the 5′ end of the genome is located at 4th base into the sequence. Thus, it is unlikely that this adenylate residue correlates to the end of the HCV subgenome in HCV replicon cells. Rather, it seems more likely that the 5′ terminal nucleotide has been converted to adenylate from guanylate during genomic replication in the replicon cells. To confirm this possibility we conducted RACE to analyze the 5′ end structure of the HCV subgenomic RNA.

First, we analyzed the 5′ end structure of the HCV subgenome in HCV replicon cells that were established by introduction of three independent HCV subgenomes with different bases at the 5′ end. We synthesized three types of HCV subgenomes by in vitro transcription; one type had an extra adenylate at the 5′ end, the second had an extra

uridylate at the 5′ end, and the third had an extra guanylate at the 5′ end. Other than this initial extra residue, the three types of subgenome had the same nucleotide sequences. After transfection of each RNA into Huh7 cells, transfected cells were selected by adding G418 to the culture medium. The clones obtained from cells transfected with each genomic RNA were pooled and expanded to about 5 million cells and the 5′ end of the HCV subgenome in each group was analyzed by RACE as described in 'Materials and Methods'. The data demonstrated that the nucleotide at each of the 5′ end of the HCV genomes was exclusively guanlyate in all HCV replicon cell lines when analyzed them at the early stage, most likely in a month, of the establishment of cell lines (fig. 3; data not shown). This is consistent with data reported previously by another group using an animal model [13]. Next, we analyzed the HCV subgenomic RNA in the HCV replicon cell lines at about 3 months after they were established. Surprisingly, the 5′ end structure of the HCV genomic RNA obtained from the cells was 5′GCC--- in 11 clones and 5′ACC--- in 18 clones.

Finding adenylate at the 5′ end of the genome suggests the possibility of some intriguing mechanism for the initiation of RNA synthesis by NS5B in HCV replicon cells. The initiation of the genome might start not only with guanylate but also with adenylate. It is also possible that the synthesis of the negative strand RNA of the HCV subgenome, in particular the incorporation of the 3′ end nucleotide, may be redundant: G:C pairing and G:U pairing may occur, interactions of which are often shown in RNA molecules such as tRNA.

NS5B has been shown to synthesize RNA in a template-dependent manner via a primer-independent (de novo) mechanism in vitro [21, 22]. During polymerization by NS5B in vitro, the kinetics of the initiation of RNA synthesis depend on the concentration of substrates, and the 3′ end sequence of the template. NS5B preferred ATP and GTP as the first initiator nucleotide for de novo RNA synthesis when the 3′ end of the HCV genome, the sequence of which is ---GU_{OH} 3′, was used as a template [21, 22]. Selection of guanylate by NS5B as an initiator nucleotide may be achieved by the formation of a basepair of guanylate with the terminal uridylate. Moreover, using various templates with different nucleotide sequences, the selection efficiency of the nucleotide at the initiation of RNA synthesis is in the order GTP>ATP≫CTP⋙UTP [23]. If the nucleotide at the 3′ end of a template is a less preferred nucleotide for NS5B in de novo synthesis of RNA, the penultimate base, if preferred by the enzyme, is used as the initiator base for synthesis of RNA. However, the fidelity of NS5B in choosing the initiation nucleotide is still unclear. Moreover, the biochemical analysis of the polymerase activity of NS5B in vitro was conducted in the presence of NS5B alone. Recent reports have demonstrated that NS5B associates with NS5A, another HCV nonstructural protein [24]. Thus, it is possible that characteristics of the enzymatic activity of NS5B may be modified by such an interaction in vivo.

^{32}P-AMP and -GMP spots detected by thin-layer chromatography co-migrated and overlapped well with authentic AMP and GMP markers (fig. 2). This evidence indicates that there is no modification on either of these nucleotides, and also strongly supports the idea that the 5′ end of the HCV genome is phosphorylated but remains free from other modifications.

Determination of the crystallographic structures of the active site domains of many RNA-dependent RNA polymerases (RdRp) has revealed an evolutionary link between HCV NS5B and the catalytic subunit of bacteriophage Φ6 RdRp, which also initiates RNA synthesis in a de novo manner [25]. According to the model of the initiation of RNA synthesis by Φ6 RNA polymerase, a base at the penultimate position at the 3′ end of the template pairs with the complementary nucleoside triphosphate. Next, a substrate basepair forms at the 3′ end base which aligns the specific binding pocket (site S) according to Butcher et al. [25]. After formation of the basepairs, these two nucleotides are covalently linked by a phosphodiester bond and the elongation process occurs. Although the authors suggested that this mechanism is applicable to the initiation reaction for de novo RNA synthesis by HCV NS5B, this conclusion is debatable [26]. Thus, more work is required to clarify the precise molecular mechanism of de novo RNA synthesis by NS5B.

As mentioned above, efficient incorporation of ^{32}P-γ-GMP into the RNA synthesized de novo by NS5B in an in vitro reaction was observed when the 3′ end of the HCV genome was used as a template. This is likely due to the formation of a basepair between guanosine triphosphate and uridylate, the base at the 3′ end of the template. It is unclear whether the formation of a G:U pair occurs between the 5′ end of the HCV genome and the 3′ end of its complementary strand in vivo. However, if such a basepair forms with some frequency, the structure of the 3′ end of the complementary strand of the genome would be changed from 3′CGG---5′ to a sequence of 3′UGG---5′. In this case, de novo synthesis of the HCV genomic RNA would start with A rather than G. Thus, detection of AMP at the 5′ end of the HCV subgenome may be explained by redundant basepairing at the 5′ end.

Nucleotide sequences of the HCV genome derived from various sources have been reported [27]. The nucleotide at the 5′ end of the HCV genome was reported to be either adenylate or guanylate, although uridylate or guanylate were also present at the end in a few cases. Adenylate residue at the 5′ end is preferred in some HCV genotypes, such as HCV-3a and HCV-2a, and a 5′ guanylate residue is preferred in other HCV genotypes, including HCV-1a and -1b. These data are significantly different from our observation that HCV genomes with guanylate or adenylate at the 5′ end are almost equally represented in Huh7 replicon cells which were established by introducing HCV subgenomic RNA of the 1b type. Although we do not know the reason for the presence of two types of HCV genome in these cells, there are at least two possibilities: (1) evolutional selection between HCV genomes with differing 5′ residues in the HCV replicon cells is negligible, and (2) the mechanism of initiation of HCV RNA synthesis in the HCV replicon cells is somehow different from the initiation of RNA synthesis in hepatocytes in vivo.

Phylogenetic analyses of the HCV genome has shown that the evolutionary distance between HCV-3a and HCV-2a is greater than the distance between HCV-3a and HCV-1b [27]. However, HCV-3a and HCV-2a have a genome containing predominantly adenylate at the 5′ end while the HCV-1b genome contains guanylate at its 5′ end. Importantly, HCV genomes incorporating guanylate or adenylate at the 5′ end are sporadically present in HCV-3a or HCV-1b, respectively. This observation, together with our findings, suggests that HCV NS5B might have had a similar ability to initiate de novo RNA synthesis with adenylate or guanylate during the early stages of its evolution. NS5B may then have gradually acquired a mechanism to select a specific initiator nucleotide in certain HCV genotypes. However, this selective mechanism may be lost when the HCV genome is replicated under in vitro conditions, such as in Huh7 cells. Clarification of the precise molecular mechanism of de novo RNA synthesis by NS5B may help to clarify this possibility.

Acknowledgements

The authors acknowledge to the member of the Department of Viral Oncology for their helps and suggestion to this work. This work was supported by Grants-in-Aid for cancer research and for the Second-term Comprehensive 10-year Strategy for Cancer Control from the Ministry of Health, Labor, and Welfare, through grants-in-aid for scientific research from the Ministry of Education, Culture, Sports, Science and Technology, Grants-in-Aid for research for the future from the Japanese Society for the Promotion of Science, and by the Program for Promotion of Fundamental Studies in Health Science of the Organization for Pharmaceutical Safety and Research (OPSR) of Japan.

References

1 Egloff MP, Benarroch D, Selisko B, Romette JL, Canard B: An RNA cap (nucleoside-2′-O-)-methyltransferase in the flavivirus RNA polymerase NS5:crystal structure and functional characterization. EMBO J 2002;21:2757–2768.
2 Lee YF, Nomoto A, Detjen BM, Wimmer E: A protein covalently linked to poliovirus genome RNA Proc Natl Acad Sci USA 1977;74:59–63.
3 Nomoto A, Detjen B, Pozzatti R, Wimmer E: The location of the polio genome protein in viral RNAs and its implication for RNA synthesis. Nature 1977;268:208–213.
4 Paul AV, van Boom JH, Filippov D, Wimmer E: Protein-primed RNA synthesis by purified poliovirus RNA polymerase. Nature 1998;393:280–284.
5 Shimotohno K: Hepatitis C virus as a causative agent of hepatocellular carcinoma. Intervirology 1995;38:162–169.
6 Tsukiyama-Kohara K, Iizuka N, Kohara M, Nomoto A: Internal ribosome entry site within hepatitis C virus RNA. J Virol 1992;66:1476–1483.
7 Wang C, Sarnow P, Siddiqui A: Translation of human hepatitis C virus RNA in cultured cells is mediated by an internal ribosome-binding mechanism. J Virol 1993;67:3338–3344.
8 Choo QL, Richman KH, Han JH, Berger K, Lee C, Dong C, Gallegos C, Coit D, Medina-Selby R, Barr PJ, et al: Genetic organization and diversity of the hepatitis C virus. Proc Natl Acad Sci USA 1991;88:2451–2455.
9 Kato N, Hijikata M, Ootsuyama Y, Nakagawa M, Ohkoshi S, Sugimura T, Shimotohno K: Molecular cloning of the human hepatitis C virus genome from Japanese patients with non-A, non-B hepatitis. Proc Natl Acad Sci USA 1990;87:9524–9528.
10 Tanaka T, Kato N, Cho MJ, Shimotohno K: A novel sequence found at the 3′ terminus of hepatitis C virus genome. Biochem Biophys Res Commun 1995;215:744–749.
11 Tanaka T, Kato N, Cho MJ, Sugiyama K, Shimotohno K: Structure of the 3′ terminus of the hepatitis C virus genome. J Virol 1996;70:3307–3312.
12 Lohmann V, Korner F, Koch J, Herian U, Theilmann L, Bartenschlager R: Replication of subgenomic hepatitis C virus RNAs in a hepatoma cell line. Science 1999;285:110–113.
13 Kolykhalov AA, Agapov EV, Blight KJ, Mihalik K, Feinstone SM, Rice CM: Transmission of hepatitis C by intrahepatic inoculation with transcribed RNA. Science 1997;277:570–574.
14 Sugiyama K, Kato N, Mizutani T, Ikeda M, Tanaka T, Shimotohno K: Genetic analysis of the hepatitis C virus (HCV) genome from HCV-infected human T cells. J Gen Virol 1997;78(Pt 2):329–336.
15 Takeuchi T, Katsume A, Tanaka T, Abe A, Inoue K, Tsukiyama-Kohara K, Kawaguchi R, Tanaka S, Kohara M: Real-time detection system for quantification of hepatitis C virus genome. Gastroenterology 1999;116:636–642.
16 Kishine H, Sugiyama K, Hijikata M, Kato N, Takahashi H, Noshi T, Nio Y, Hosaka M, Miyanari Y, Shimotohno K: Subgenomic replicon derived from a cell line infected with the hepatitis C virus. Biochem Biophys Res Commun 2002;293:993–999.

17 Miyanari Y, Hijikata M, Yamaji M, Hosaka M, Takahashi H, Shimotohno K: Hepatitis C virus Non-structural proteins in the probable membranous compartment function in viral RNA replication. J Biol Chem 2003;278: 50301–50308.
18 Lohmann V, Korner F, Dobierzewska A, Bartenschlager R: Mutations in hepatitis C virus RNAs conferring cell culture adaptation. J Virol 2001;75:1437–1449.
19 Krieger N, Lohmann V, Bartenschlager R: Enhancement of hepatitis C virus RNA replication by cell culture-adaptive mutations. J Virol 2001;75:4614–4624.
20 Nomoto A, Kitamura N, Golini F, Wimmer E: The 5′-terminal structures of poliovirion RNA and poliovirus mRNA differ only in the genome-linked protein VPg. Proc Natl Acad Sci USA 1977;74:5345–5349.
21 Zhong W, Uss AS, Ferrari E, Lau JY, Hong Z: De novo initiation of RNA synthesis by hepatitis C virus nonstructural protein 5B polymerase. J Virol 2000;74:2017–2022.
22 Kim M, Kim H, Cho SP, Min MK: Template requirements for de novo RNA synthesis by hepatitis C virus nonstructural protein 5B polymerase on the viral X RNA. J Virol 2002;76: 6944–6956.
23 Lohmann V, Roos A, Korner F, Koch JO, Bartenschlager R: Biochemical and structural analysis of the NS5B RNA-dependent RNA polymerase of the hepatitis C virus. J Viral Hepatol 2000;7:167–174.
24 Shirota Y, Luo H, Qin W, Kaneko S, Yamashita T, Kobayashi K, Murakami S: Hepatitis C virus (HCV) NS5A binds RNA-dependent RNA polymerase (RdRP) NS5B and modulates RNA-dependent RNA polymerase activity. J Biol Chem 2002;277:11149–11155.
25 Butcher SJ, Grimes JM, Makeyev EV, Bamford DH, Stuart DI: A mechanism for initiating RNA-dependent RNA polymerization. Nature 2001;410:235–240.
26 O'Farrell D, Trowbridge R, Rowlands D, Jager J: Substrate complexes of hepatitis C virus RNA polymerase (HC-J4): Structural evidence for nucleotide import and de-novo initiation. J Mol Biol 2003;326:1025–1035.
27 HCV database: http://s2as02.genes.nig.ac.jp/index.html

THE JOURNAL OF BIOLOGICAL CHEMISTRY
Vol. 280, No. 18, Issue of May 6, pp. 18355–18360, 2005
Printed in U.S.A.

Role of Cyclophilin B in Activation of Interferon Regulatory Factor-3*

Received for publication, February 14, 2005
Published, JBC Papers in Press, March 10, 2005, DOI 10.1074/jbc.M501684200

Yoko Obata‡, Kazuo Yamamoto‡, Masanobu Miyazaki‡, Kunitada Shimotohno§, Shigeru Kohno‡, and Toshifumi Matsuyama‡¶

From the ‡Department of Molecular Microbiology and Immunology, Nagasaki University Graduate School of Biomedical Sciences, 1-12-4 Sakamoto, Nagasaki 852-8523 and the §Department of Viral Oncology, Institute for Virus Research, Kyoto University, Sakyo-ku, Kyoto 606-8507, Japan

IRF-3 is a member of the interferon regulatory factors (IRFs) and plays a principal role in the induction of interferon-β (IFN-β) by virus infection. Virus infection results in the phosphorylation of IRF-3 by IκB kinase ε and TANK-binding kinase 1, leading to its dimerization and association with the coactivators CREB-binding protein/p300. The IRF-3 holocomplex translocates to the nucleus, where it induces IFN-β. In the present study, we examined the molecular mechanism of IRF-3 activation. Using bacterial two-hybrid screening, we isolated molecules that interact with IRF-3. One of these was cyclophilin B, a member of the immunophilins with a *cis-trans* peptidyl-prolyl isomerase activity. A GST pull-down assay suggested that one of the autoinhibition domains of IRF-3 and the peptidyl-prolyl isomerase domain of cyclophilin B are required for the binding. A knockdown of cyclophilin B expression by RNA interference resulted in the suppression of virus-induced IRF-3 phosphorylation, leading to the inhibition of the subsequent dimerization, association with CREB-binding protein, binding to the target DNA element, and induction of IFN-β. These findings indicate that cyclophilin B plays a critical role in IRF-3 activation.

Interferon regulatory factors (IRF(s))[1] are a family of transcription factors that regulate a variety of biological events, including innate immunity. Once activated by the invasion of a pathogen, such as viruses and bacteria, IRFs regulate the expression of various genes encoding immunomodulatory cytokines and chemokines and limit the spread of infection. Among these factors, interferons (IFNs) play important roles in host defense, cell growth regulation, and immune activation (1, 2). IFNs include the type I IFN-αs and IFN-β and the type II IFN-γ. Type I IFNs are immediately induced in response to various viral infections, and IRF-3 and IRF-7 play an important role in their induction (3, 4). The mode of IRF-3 involvement against virus infection has been analyzed by using Newcastle disease virus (NDV) and Sendai virus (5–9). IRF-3 is expressed in the cytoplasm as a latent, inactive form, and its C-terminal serine/threonine residues are phosphorylated by IκB kinase ε and TANK-binding kinase 1 (10, 11). Virus-induced C-terminal phosphorylation of IRF-3 represents an important posttranslational modification, leading to dimerization (6, 7), translocation from the cytoplasm to the nucleus, association with CBP/p300 coactivators (6, 9), stimulation of DNA binding to the IFN-stimulated response elements (ISREs), and activation of the corresponding genes (5, 8, 9).

IRF-3 consists of an N-terminal DNA-binding domain that specifically binds to an ISRE motif, and a C-terminal IRF association domain (IAD) that mediates protein-protein interactions. IRF-3 uses the IAD for both intramolecular autoinhibition interactions and intermolecular dimerizations (6, 12). Furthermore, IRF-3 possesses a transactivation domain (amino acids 134–394) and two autoinhibition domains found within the proline-rich sequence (amino acids 134–197) and at the C-terminal end (amino acids 407–414). The two autoinhibition domains are thought to interact with each other to generate a closed conformation that masks the C-terminal IAD, the DNA-binding domain, and the nuclear localization signal of IRF-3, which prevents homodimerization and DNA binding in uninfected cells. The C-terminal phosphorylation of IRF-3 might open the conformation, leading to dimer formation and exposure of the nuclear localization signal and the DNA-binding domain (6, 13, 14). However, the molecular events associated with such a drastic conformational change remain unknown. In the present study, we demonstrate the interaction of IRF-3 with cyclophilin B (CypB), an immunophilin with *cis-trans* peptidyl-prolyl isomerase and chaperone-like activities (15). The knockdown of CypB by RNA interference prevented the NDV-induced IRF-3 phosphorylation, dimerization, association with CBP, binding to the ISRE, and induction of IFN-β.

EXPERIMENTAL PROCEDURES

Bacterial Two-hybrid Screening—A BacterioMatch™ two-hybrid SystemXR Plasmid cDNA library (Stratagene, La Jolla, CA) was used to screen IRF-3 interacting proteins according to the manufacturer's protocol. For the construction of the bait plasmid, the GST fusion expression plasmid pGEX-IRF-3 was digested at the NcoI site, which overlapped with the initiation codon of IRF-3, filled in with the Klenow fragment of DNA polymerase I, and then digested by XhoI. The plasmid pBT was digested by BamHI, filled in with the Klenow fragment of DNA polymerase I, and then digested by XhoI. The NcoI/Klenow-XhoI fragment containing the IRF-3 coding region was ligated with the pBT fragment. The junction of the cloning site of the resultant plasmid pBT-IRF-3 was verified by sequencing. Competent cells of the BacterioMatch two-hybrid system *Escherichia coli* reporter strain were transformed with pBT-IRF-3, together with the pTRG-cDNA library (Human HeLa cell plasmid cDNA library, number 982208, Stratagene). As every

* This work was supported by a grant-in-aid from the Ministry of Education, Culture, Sports, Science, and Technology and by the 21st Century Center of Excellence Program of Nagasaki University. The costs of publication of this article were defrayed in part by the payment of page charges. This article must therefore be hereby marked "*advertisement*" in accordance with 18 U.S.C. Section 1734 solely to indicate this fact.

¶ To whom correspondence should be addressed. Tel.: 81-95-849-7081; Fax: 81-95-849-7083; E-mail: tosim@net.nagasaki-u.ac.jp.

[1] The abbreviations used are: IRF, interferon regulatory factor; IFN, interferon; CBP, cAMP-response element-binding protein-binding protein; ISRE, interferon-stimulated response element; NDV, Newcastle disease virus; ISG, interferon-stimulated gene; GST, glutathione *S*-transferase; CypB, cyclophilin B; PPIase, peptidyl-prolyl isomerase; siRNA, small interfering RNA.

transformation produced 4.0–5.0 × 10^5 clones, we finally screened 4.30 × 10^6 colonies after 10 transformations. The cDNA-containing plasmids were recovered from the antibiotic-resistant and *lac*Z-positive clones, and the sequences of the cDNA inserts were verified, using the pTRG forward primer (5′-CAGCCTGAAGTGAAAGAA-3′) and the pTRG reverse primer (5′-ATTCGTCGCCCGCCATAA-3′), by a PRISM 310 or 3100 autosequencer. For the construction of the N-terminal Myc-tag fusion protein expression vector, a synthetic oligonucleotide containing the Myc-tag sequence, followed by HindIII, NcoI, BamHI, NotI, and EcoRI sites as multicloning sites, was ligated into pcDNA3 digested with HindIII and EcoRI to yield the plasmid pcDNA/Myc. The cDNAs of the candidate positive clones were amplified by PCR with the pTRG forward and reverse primers, digested with BamHI, NotI, or EcoRI for the 5′-junction and XhoI for the 3′-junction, and then subcloned into the corresponding sites of pcDNA3/Myc.

GST Pull-down Assay—The Myc-tagged protein encoded by the cloned cDNA was synthesized by the TNT Quick Coupled Transcription/Translation Systems (Promega) with unlabeled methionine. To construct the plasmids pGEX-hIRF-3ΔN1–3, pGEX-hIRF-3 was digested with ScaI, MscI, or BglII, blunt-ended with the Klenow enzyme, and then digested with SacII. The 938-bp ScaI-SacII fragment, the 608-bp MscI-SacII fragment, and the 350-bp BglII-SacII fragment were excised and subcloned into the blunt-ended NcoI site and the SacII site of the pGEX-hIRF-3 plasmid, respectively. To construct pGEX-hIRF-3ΔC1, the 5925-bp BglII-NotI fragment of pGEX-hIRF-3 was blunt-ended with the Klenow enzyme, and then self-ligated. To construct pGEX-hIRF-3ΔC2 and -ΔC3, the 724-bp NcoI-*Mse*I fragment and the 394-bp NcoI-ScaI fragment were excised from pGEX-hIRF-3 and then subcloned into the blunt-ended NotI site and the NcoI site of the pGEX-hIRF-3 plasmid, respectively. To create a PPIase-defective mutant of CypB, both the arginine at the 96th position and the phenylalanine at the 101st position of CypB were substituted by alanine, using the QuikChange site-directed mutagenesis kit (Stratagene). To construct the Myc-cyclophilin A (CypA) expression plasmid, the CypA cDNA was amplified by RT-PCR using PfuUltra™ DNA polymerase and the gene-specific primers (forward 5′-CGGAATTCGGCACGAGGCCATGGTCAACCCCACC-GTGTTC-3′ and reverse 5′-GCCGCTCGAGTCAAACTTATTCGAGTT-GTCCACAG-3′) with an amplification cycle of 95 °C/30 s, 62 °C/30 s and 72 °C/60 s for 25 cycles. The amplified cDNA was digested with EcoRI and XhoI, and was subcloned into the corresponding sites of pcDNA3-Myc-CypB. *E. coli* strain TG1 was transformed with each plasmid construct, and was grown in LB medium to an $A_{600} > 0.4$. After 3 h of culture in the presence of 2 mM IPTG, for the induction of fusion protein synthesis, the cells were harvested by centrifugation, resuspended in one-twelfth volume of PBS(-) containing 0.5 mM phenylmethylsulfonyl fluoride, and sonicated. The amount of protein used was adjusted on the basis of an SDS-PAGE analysis. The cleared lysates were mixed with 20 μl of glutathione-Sepharose beads for 1 h at 4 °C and subsequently were washed 3 times with DBT-0.1 (dilution buffer with Triton X) (20 mM Hepes-KOH (pH 7.9), 0.5 mM EDTA, 1 mM dithiothreitol, 20% glycerol, 0.2% Triton X-100, 100 mM KCl). The affinity beads were incubated with 150 μl of precleared *in vitro* translated protein for 2 h at 4 °C. After washing the beads 3 times with DBT-0.4 (20 mM Hepes-KOH (pH 7.9), 0.5 mM EDTA, 1 mM dithiothreitol, 20% glycerol, 0.2% Triton X-100, 400 mM KCl), the proteins retained on the beads were extracted in 20 μl of SDS-PAGE sample buffer and were separated on 4–20% SDS gradient gels (Daiichi Chemicals, Tokyo, Japan). Proteins were detected by Western blotting with a rabbit polyclonal anti-Myc antibody (Cell Signaling Technology).

Immunoprecipitation—To detect the association of endogenous IRF-3 and CypB, we performed the immunoprecipitation experiment using the human fibrosarcoma cell line, HT1080. The aliquot of cells was pelleted by centrifugation and infected with NDV for 10 min at 37 °C, and then a whole cell extract was prepared. An aliquot of each extract was incubated with 5 μg of goat IgG or goat polyclonal anti-IRF-3 antibody (C-20, Santa Cruz Biotechnology, Santa Cruz, CA) for 1 h at 4 °C. After this incubation, the protein G beads were added to the mixture and incubated for 4 h at 4 °C. The following procedures were the same as those used for the GST pull-down described above. Proteins were detected by Western blotting with a goat polyclonal anti-IRF-3 antibody (C-20) and a rabbit polyclonal anti-cyclophilin B antibody (Affinity BioReagents. Inc.).

RNA Interference—Human fibrosarcoma HT1080 cells were maintained in Dulbecco's modified Eagle's medium supplemented with 10% fetal bovine serum, 100 μg/ml penicillin, and 50 μg/ml streptomycin in a 37 °C incubator with 5% CO_2 and 100% humidity. The sense and antisense strands of the siRNAs for CypB (5′-GGUGGAGAGCAC-CAAGACATT-3′, 5′-UGUCUUGGUGCUCUCCACCTT-3′) and for the control (5′-ACAGAACCACGAGAGGUGGTT-3′, 5′-CCACCUCU-CGUGGUUCUGUTT-3′) were annealed according to the provider's instructions, respectively (JBioS, Tokyo, Japan). Cells were transfected with siRNAs using Lipofectamine 2000 (Invitrogen). In brief, 1.0 × 10^5 cells/well were seeded in a 6-well tissue culture plate. After 24 h of incubation, the medium was replaced by culture medium without antibiotics. To allow the siRNA-liposome complexes to form, 5 μl of siRNAs (20 μM) and 5 μl of Lipofectamine 2000 reagent were combined in 500 μl of Opti-MEM medium and incubated at room temperature for 20 min. This mixture was added to the cells and incubated for 24 h. The cells were then washed twice with dilution medium (Dulbecco's modified Eagle's medium containing 10% bovine serum albumin) and infected with NDV by the addition of 100 μl of allantoic fluid from NDV-infected chicken eggs (1000 hemagglutinin units/ml) for 1.5 h. After washing twice with complete medium (Dulbecco's modified Eagle's medium supplemented with 10% fetal bovine serum, 100 μg/ml penicillin, and 50 μg/ml streptomycin), the cells were further incubated in complete medium for 10.5 h before harvesting for extract preparation.

Preparation of Whole Cell Extracts—The cells were washed with ice-cold phosphate-buffered saline(−) and then scraped and suspended in 400 μl of cell lysis buffer (50 mM Tris-HCl (pH 8.0), 120 mM NaCl, 0.5% Nonidet P-40, 10% glycerol, 2 mM Na_3VO_4, 10 mM NaF, 0.2 mM phenylmethylsulfonyl fluoride). The cells were lysed by vortexing briefly, and the lysates were incubated on ice for 10 min. The whole cell extracts were recovered after centrifugation at 15,000 rpm for 10 min at 4 °C.

Western Blotting—The procedures were the same as those used in the GST pull-down experiment described above. The antibodies used were the goat polyclonal anti-IRF-3 antibody (C-20), the mouse monoclonal anti-IRF-3 Ser(P)-396 antibody (HIS5133, a gift provided by Drs. J. Hiscott and M. Servant, McGill University), the rabbit polyclonal anti-cyclophilin B antibody, and the mouse monoclonal anti-actin antibody (Chemicon).

Native PAGE Assay—The native PAGE assay was performed by using 7.5% polyacrylamide gels (Daiichi Chemicals). The gel was prerun in a running buffer containing 25 mM Tris and 192 mM glycine, with and without 1% deoxycholate in the cathode and anode chambers, respectively, for 30 min at 40 mA. Aliquots of whole cell extracts were diluted in native sample buffer (62.5 mM Tris-HCl (pH 6.8), 15% glycerol, and 1% deoxycholate), applied to the gel, and electrophoresed for 60 min at 25 mA. Immunoblotting was performed as described above. Proteins were detected by Western blotting with a goat polyclonal anti-IRF-3 antibody (C-20) or a rabbit polyclonal anti-IRF-3 Ser(P)386 antibody (IBL).

Electrophoretic Mobility Shift Assay—To examine the binding of IRF-3 to the IFN-β promotor, an electrophoretic mobility shift assay was performed using whole cell extracts from siRNA-transfected and NDV-infected or -uninfected HT1080 cells. The extracts were incubated in a reaction buffer (25 mM Tris-HCl (pH 8.0), 60 mM NaCl, 0.25% Nonidet P-40, 5% glycerol, 1 mM Na_3VO_4, 5 mM NaF, 1 mM dithiothreitol, 100 mg/ml poly(dI-dC)). After a 30-min incubation on ice, ~10,000 cpm of a ^{32}P-labeled double-stranded oligonucleotide containing the ISRE sequence of the ISG15 gene (5′-GGGAAAGGGAAACCGAAACT-GAA-3′) were added to the reactions, which were then incubated for an additional 30 min at 25 °C. The reactions were further incubated with an anti-IRF-3 antibody (C-20) or an anti-CBP antibody (A-22X) (Santa Cruz Biotechnology) for 30 min at 25 °C. The binding reactions were mixed with 1 μl of loading buffer (0.1% bromphenol blue in the same buffer used for the binding reactions) and then were electrophoresed on a nondenaturing 4% polyacrylamide gel with 0.5 × TBE (Tris borate-EDTA) at 200 V for 2 h. The gel was dried and analyzed by an image analyzer, BAS5000 (Fuji, Tokyo).

Chromatin Immunoprecipitation Assay—HT1080 cells were mock- or NDV-infected for 12 h and then treated with formaldehyde to cross-link the proteins bound to DNA. The cross-linked proteins were purified and immunoprecipitated with the anti-IRF-3 antibody (C-20). After reversal of the cross-linking, the DNA was amplified using primers for the ISG15 promoter (5′-TTTTCCCTGTCTTTCGGTCATTCG-3′, 5′-TAT-TATAAGCCTGAGGCACACACG-3′) with an amplification cycle of 94 °C/1 min, 55 °C/1 min, and 72 °C/2 min for 30 cycles.

Enzyme-linked Immunosorbent Assay for IFN-β—The amounts of human IFN-β in the culture medium supernatants before and after NDV infection were quantified with a human interferon-β enzyme-linked immunosorbent assay kit (R&D Systems). Data are expressed as the mean ± S.D. Differences among groups were examined for statistical significance using one-factor analysis of variance (Bonferroni/Dunn). A p value < 0.05 denoted the presence of a statistically significant difference.

RESULTS

Isolation of Putative IRF-3-binding Proteins by the Bacterial Two-hybrid Screening—To isolate the protein(s) that associate with IRF-3, we performed a screening by a bacterial two-hybrid system (16, 17). The bait was fused to the full-length bacteriophage λ repressor protein (λ*cI*), whereas the corresponding target protein was fused to the N-terminal domain of the α-subunit of RNA polymerase. When the bait and target interact, they recruit and stabilize the binding of RNA polymerase at the promoter and activate the transcription of reporter genes, the carbenicillin-resistance and the β-galactosidase genes. In addition, this system offers the ability to detect an interaction between a pair of protein domains with an equilibrium dissociation constant in the high nanomolar range. In the present study, we used IRF-3 as the bait and a human HeLa cell cDNA library as the target. We obtained 272 antibiotic-resistant and *lac*Z-positive clones from 4.30×10^6 screened clones. To identify the protein encoded by the candidate positive clones, the nucleotide sequence of each clone was determined. Among the clones obtained, only 25 clones encoded in-frame fusion proteins to the λ*cI* repressor. These clones were used in a search for homology in the NCBI data base. The cDNA fragments of the positive clones were subcloned into an expression vector to produce N-terminally Myc-tagged fusion proteins. However, we obtained *in vitro* coupled transcription/translation products from only 13 of 25 clones. For these 13 clones, we performed a GST pull-down assay to confirm their binding activities to IRF-3. Only clone A25 (cyclophilin B) showed specific binding to IRF-3 (data not shown). Therefore, we concentrated our efforts on the interaction between IRF-3 and CypB.

Mapping the IRF-3 and Cyclophilin B Interaction Domains—To confirm the specificity of the interaction between IRF-3 and CypB, we examined which region of IRF-3 is important for binding to CypB. A GST pull-down assay was performed with a series of IRF-3 deletion mutants fused to GST and *in vitro* translated full-length CypB (Fig. 1*A*). As mentioned above, CypB bound to GST-IRF-3 but not to GST alone (Fig. 1*B*, *lanes 3* and *2*). The deletion of the N-terminal DNA-binding domain somehow enhanced the binding of CypB (Fig. 1*B*, *lane 4*), whereas further removal of the nuclear export signal and the proline-rich region reduced the affinity to CypB (*lane 5*). Unexpectedly, the deletion of the IAD restored the interaction potential of IRF-3 to CypB (Fig. 1*B*, *lane 6*). When we removed the C-terminal 296 residues from IRF-3, the interaction with CypB was not detected (Fig. 1*B*, *lane 9*). It is noteworthy that the mutants ΔN3 and ΔC1 do not share any regions of IRF-3 but still exhibited the CypB binding, suggesting that IRF-3 has multiple sites for CypB binding. Furthermore, the IAD seems to have an inhibitory effect on the binding, as the binding of ΔN2 is weaker than that of ΔN3, the construct lacking two thirds of the IAD from ΔN2. We did not perform a GST pull-down analysis with GST-CypB to detect the binding with IRF-3, because the GST-CypB expression plasmid failed to produce a detection level of the protein in *E. coli*.

Next, we examined the regions of CypB required for the interaction with IRF-3. Because CypB is a rather small protein (208 amino acids), even a small deletion drastically destabilized the mutant forms of the protein (data not shown). Thus, we tested whether the PPIase activity of CypB, a well known biological activity of the protein, was required for the binding to IRF-3. For this purpose, arginine 96 and phenylalanine 101 in the PPIase domain of CypB were substituted with alanines by site-directed mutagenesis (Fig. 1*C*). As shown in Fig. 1*D*, the PPIase mutant did not bind to IRF-3 (*lane 9*). In addition, we found that cyclophilin A (CypA), the most abundant cyclophilin *in vivo*, could not bind to IRF-3 (*lane 3*).

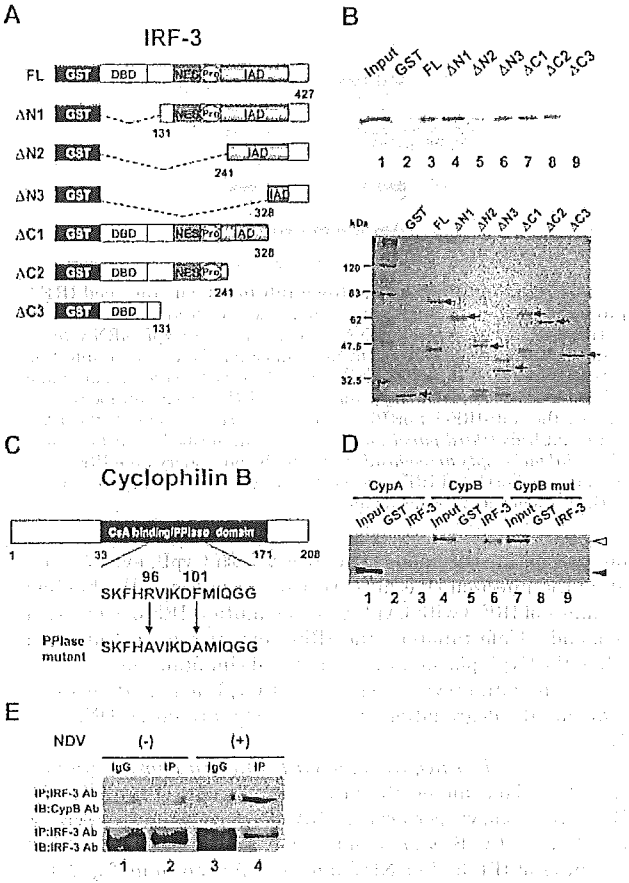

FIG. 1. **Mapping the interaction domains of IRF-3 and CypB.** *A*, schematic representation of IRF-3 deletion mutants. Structures of wild type (*top*) and deletion mutants (ΔN1–3 and ΔC1–3) of IRF-3 are shown. Locations of functional domains are indicated. *DBD*, DNA-binding domain; *NES*, nuclear export signal; *Pro*, proline-rich region; *IAD*, interferon-associated domain. *B*, GST pull-down assay between IRF-3 mutants and CypB. *Input*, 5% of *in vitro* translated Myc-tagged CypB was included in the binding reactions. *GST*, GST protein only (not fused with IRF-3); *FL*, GST fusion of wild type IRF-3 protein; *ΔN1*, GST fusion of IRF-3 truncated 131 residues from the N terminus; *ΔN2*, GST fusion of IRF-3 truncated 241 residues from the N terminus; *ΔN3*, GST fusion of IRF-3 truncated 328 residues from the N terminus; *ΔC1*, GST fusion of IRF-3 truncated 99 residues from the C terminus; *ΔC2*, GST fusion of IRF-3 truncated 186 residues from the C terminus; *ΔC3*, GST fusion of IRF-3 truncated 296 residues from the C terminus. *C*, schematic representation of cyclophilin B PPIase mutants. The wild type CypB structure (*top*) is shown. The amino acid sequence of the wild type CypB and the mutated residues are shown. *CsA*, Cyclosporin A. *D*, GST pull-down assay between CypB, CypB PPIase mutant, or CypA and wild type IRF-3. *Input*, 5% of *in vitro* translated Myc-tagged CypB, Myc-tagged CypB PPIase mutant, or Myc-tagged CypA was included in the binding reactions, respectively. *GST*, GST protein only (not fused with IRF-3); *IRF-3*, GST-fusion of wild type IRF-3 protein. The *solid* and *empty arrowheads* indicate CypB and CypA, respectively. *E*, co-immunoprecipitation assay to detect an endogenous association between IRF-3 and CypB *in vivo*. Whole cell lysates prepared from cells, either mock-infected or NDV-infected for 10 min, were used as the input. *IgG*, lysates incubated with goat IgG (*lanes 1* and *3*) *IP*, lysates incubated with goat polyclonal anti-IRF-3 antibody (C-20) (*lanes 2* and *4*). *IB*, immunoblot. The data are representative of three independent experiments.

Then, we examined the interaction between IRF-3 and CypB *in vivo*. The association of endogenous IRF-3 and CypB was detected when an anti-IRF-3 antibody was used for the precipitation of an extract prepared 10 min after NDV infection (Fig. 1*E*, *lane 4*) but not 30 min after the infection (data not shown). On the other hand, the available anti-CypB antibodies could

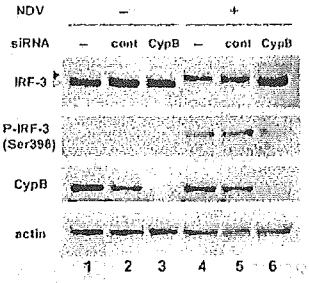

FIG. 2. **Cyclophilin B knockdown inhibits virus-induced IRF-3 phosphorylation.** HT1080 cells were mock-transfected (*lanes 1* and *4*) or transfected with control siRNA (*lanes 2* and *5*) or CypB siRNA (*lanes 3* and *6*), respectively, followed by mock infection (*lanes 1–3*) or infection with NDV for 12 h (*lanes 4–6*). Whole cell extracts were prepared and subjected to immunoblotting using the anti-IRF-3 (C-20) antibody (*first panel*), the anti-IRF-3 Ser(P)-396 antibody (*second panel*), the anti-CypB antibody (*third panel*), or the anti-actin antibody (*fourth panel*). The *solid* and *empty arrowheads* indicate the phosphorylated IRF-3 and the unphosphorylated IRF-3, respectively. The data are representative of three independent experiments.

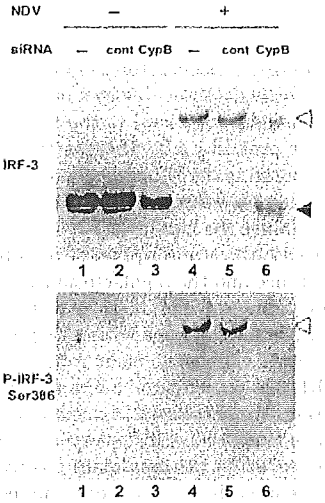

FIG. 3. **Cyclophilin B knockdown inhibits virus-induced IRF-3 dimerization.** Whole cell extracts were prepared as described in Fig. 2 and were analyzed by native PAGE followed by immunoblotting with the anti-IRF-3 (C-20) antibody (*upper panel*) and the anti-IRF-3 Ser(P)-386 antibody (*lower panel*). The *solid* and *empty arrowheads* indicate the monomer and the dimer of IRF-3, respectively. The data are representative of three independent experiments.

not precipitate the endogenous IRF-3 with CypB, even 10 min after the infection. We also tried to characterize the binding domains of IRF-3 with CypB by using mutant IRF-3 expression plasmids. Unfortunately, the IRF-3 expression was inhibited when the CypB plasmid was introduced simultaneously. This is consistent with previous reports that CypB may participate in inducing the degradation of exogenously introduced DNA (18, 19).

Cyclophilin B Is Required for Virus-induced Phosphorylation of IRF-3—To examine the physiological roles of CypB in the IRF-3 function, we performed RNA interference experiments to knock down CypB *in vivo* and then examined the biochemical activities of IRF-3 after NDV infection. As shown in Fig. 2, the expression of CypB was almost completely suppressed by the specific siRNA interference (*lanes 3* and *6*, *third panel*). NDV infection in the mock- or control siRNA-transfected cells resulted in a mobility shift of IRF-3, which reflected the C-terminal phosphorylation of IRF-3 (Fig. 2, *lanes 4* and *5*, *first panel*) (9, 20). However, IRF-3 showed an intermediate mobility in CypB siRNA-transfected/NDV-infected cells (Fig. 2, *lane 6*, *first panel*). When the same blot was reprobed with an antibody that specifically recognized a phosphorylated form of IRF-3 (21), we found that the amounts of phosphorylated IRF-3 (phosphorylated Ser-396) were reduced in the CypB siRNA-transfected cells, as compared with the mock- or control siRNA-transfected cells (Fig. 2, compare *lanes 6* with *lanes 4* and *5*, *second panel*). These results strongly suggest that the knockdown of CypB resulted in the defect in IRF-3 phosphorylation by virus infection.

The Cyclophilin B Knockdown Inhibited Virus-induced IRF-3 Dimerization—It is known that the phosphorylation of IRF-3 is prerequisite for the dimerization of IRF-3 (7, 20). We thus examined the virus-induced dimerization of IRF-3 in siRNA-transfected cells. To do this, we used the native PAGE assay that sensitively detects the difference between the monomer and dimer forms of IRF-3 (22). IRF-3 existed as a monomer in the mock-, control siRNA-, and CypB siRNA-transfected cells in the absence of NDV infection (Fig. 3, *lanes 1–3*). Upon viral infection, the monomer signals were reduced, but newly formed dimer signals were detected in the mock- and control siRNA-transfected cells (Fig. 3, *lanes 4* and *5*). However, significant amounts of the IRF-3 monomer still remained in the CypB siRNA-transfected/NDV-infected cells (Fig. 3, *lane 6*). These results clearly indicated that the specific knockdown of CypB by RNA interference inhibited the IRF-3 dimer formation induced by viral infection. The importance of CypB was again demonstrated in the phosphorylation of Ser-386, which is the critical residue in IRF-3 activation (23). CypB siRNA-transfected/NDV-infected cells failed to phosphorylate Ser-386 (Fig. 3, *panel 2*, *lane 6*).

The Cyclophilin B Knockdown Inhibited IRF-3 Binding to the ISRE and Association with CBP—Phosphorylated IRF-3 undergoes homodimerization (6, 7) and associates with the coactivators CBP/p300 (6, 9). The holocomplex has the ability to specifically recognize the target DNA sequence, called the ISRE (5, 8, 9). We examined the effects of CypB on IRF-3 in terms of the DNA binding to the ISRE and the association with the CBP/p300 coactivator, using electromobility shift assay. In the absence of NDV infection, no DNA-protein complex was observed in the mock-, control siRNA-, and CypB siRNA-transfected cells (Fig. 4, *lanes 1*, *6*, and *11*). NDV infection induced the formation of a DNA-protein complex bound to the ISRE of the ISG15 gene in the mock- and control siRNA-transfected cell extracts (Fig. 4, *lanes 2* and *7*). The addition of specific antibodies against IRF-3 to the binding reactions reduced the amount of the complex band and the induction of supershifted bands, indicating that the complex contained IRF-3 (Fig. 4, *lanes 3* and *8*). The addition of specific antibodies against CBP to the binding reactions reduced the amount of the complex but did not induce the formation of supershifted bands, indicating that complex formation was partly blocked by the antibody (Fig. 4, *lanes 4* and *9*). This is consistent with the previous result that CBP/p300 is involved in the holocomplex of IRF-3 (6–9). However, the knockdown of CypB severely impaired the DNA binding activity of IRF-3 (Fig. 4, *lane 12*). Thus, the inhibition of CypB also resulted in reduced holocomplex formation, which is required for the target gene activation by IRF-3. A chromatin immunoprecipitation analysis showed the *in vivo* binding of IRF-3 to the ISG15 promoter in NDV-infected cells (Fig. 4*B*, *lane 8*) but not in uninfected cells (Fig. 4*B*, *lane 2*). When NDV-infected cells were pretreated with CypB siRNA, the binding was significantly reduced, and no band was detected after 30 PCR cycles (Fig. 4*B*, *lane 12*), although a band was visible after 40 cycles (data not shown). The control siRNA could not reduce the binding (Fig. 4*B*, *lane 10*).

The Cyclophilin B Knockdown Reduced IFN-β Production by Newcastle Disease Virus Infection—Finally, we examined the

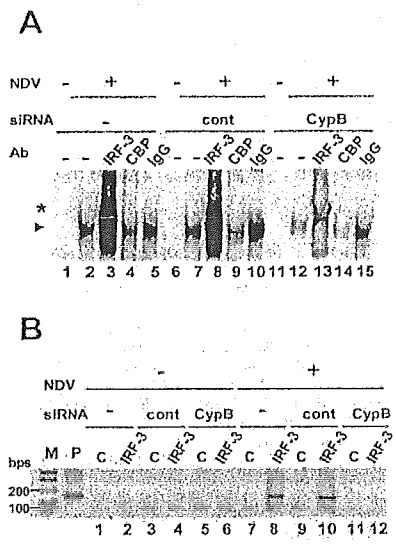

FIG. 4. **Cyclophilin B knockdown inhibits IRF-3 binding to the ISRE and association with CBP.** *A*, whole cell extracts were prepared as described in Fig. 2, and were subjected to electromobility shift assay, using the ISRE of the ISG15 gene as a probe, in the absence (*lanes 1, 2, 6, 7, 11,* and *12*) or presence of the anti-IRF-3 (C-20) antibody (*lanes 3, 8,* and *13*), the anti-CBP antibody (*Ab*) (*lane 4, 9,* and *14*), or control (*cont*) IgG (*lanes 5, 10,* and *15*). The *arrowhead* indicates the IRF-3-containing complex. The *asterisk* indicates the bands supershifted by the anti-IRF-3 antibody. *B*, chromatin immunoprecipitation assay to assess the amounts of IRF-3 bound to ISG15 promoter. *M*, marker; *P*, positive control of genomic DNA. Whole cell extracts prepared as described in Fig. 2 were subjected to the assay, using the promoter region of the ISG15 gene as primers. Each extract was immunoprecipitated with the control IgG (*C*) (*lanes 1, 3, 5, 7, 9,* and *11*) or the anti-IRF-3 (C-20) antibody (*lanes 2, 4, 6, 8, 10,* and *12*). The data are representative of three independent experiments.

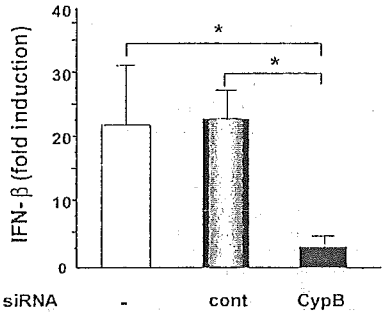

FIG. 5. **Cyclophilin B knockdown reduces IFN-β production by Newcastle Disease Virus infection.** HT1080 cells were mock-transfected, or transfected with control siRNA or CypB siRNA. After 24 h, the cells were infected with NDV for 12 h. The supernatants before and after NDV infection were analyzed by an IFN-β enzyme-linked immunosorbent assay. The results shown are the averages of three independent experiments, with S.E. *bars*. The *asterisk* indicates a p value < 0.05.

effect of CypB on the regulation of IFN-β production. The amount of IFN-β in the culture medium was assayed by enzyme-linked immunosorbent assay, before and after NDV infection. The virus infection induced a more than 25-fold activation of IFN-β in the mock- and the control siRNA-transfected cells. The CypB-siRNA treatment caused a severe defect in the viral-dependent activation of IFN-β. (Fig. 5). These results indicate that CypB is required for the efficient activation of IFN-β production upon viral infection.

DISCUSSION

We have described a novel interaction between IRF-3 and CypB. The present *in vitro* analysis suggests that autoinhibition domain of IRF-3 and the catalytic domain bearing the peptidyl-prolyl isomerase activity of CypB are required for the interaction.

CypB, a member of the cyclophilins, possesses a *cis-trans* peptidyl-prolyl isomerase activity (15). Via their PPIase activity, cyclophilins facilitate protein folding and have been shown to contribute to the maturation and trafficking of several proteins (24). Furthermore, cyclophilins regulate signal transduction cascades, as revealed by their modulation of transforming growth factor-β signaling and the transactivation of c-myb and IRF-4 (25, 26). Among the cyclophilins, CypB is distinguished from the others by the presence of an endoplasmic reticulum-directed signal sequence (15). However, CypB is found not only in the endoplasmic reticulum but also in the extracellular space and the nucleus (15). CypB has been reported to interact with prolactin. The proximal action of prolactin is mediated by its cell surface receptor. PRL activity, however, is also associated with the internalization and translocation of this hormone into the nucleus. To retrotransport it to the nucleus, and to potentiate prolactin-induced proliferation, the interaction with CypB with its PPIase activity is essential (27, 28). Similar to the interaction with prolactin, the PPIase domain of CypB is required for IRF-3 binding in a GST pull-down assay. We also found that retaining either one of the autoinhibition domains of IRF-3 is required for the binding. Previously, Mamane *et al.* (29) reported the interaction between IRF-4, a member of the IRFs, and FKBP52, another member of the immunophilins. They demonstrated that IRF-4 would not co-immunoprecipitate with FKBP52 unless the C-terminal autoinhibition domain of IRF-4 was removed. This observation raises the possibility that the interactions of immunophilins with IRF family proteins are sensitive to the conformations or the ternary structures of IRFs.

As demonstrated by our RNA interference analysis, the specific knockdown of CypB *in vivo* resulted in the inhibition of virus-induced IRF-3 activation. This was confirmed at multiple steps, including phosphorylation, dimerization, DNA binding, coactivator binding, and IFN-β-induction. If the phosphorylation of IRF-3 is a prerequisite for the following events after the virus-induced activation of IRF-3, then it is likely that CypB is involved in the phosphorylation reaction of IRF-3. The early involvement of CypB is supported by the notion that the *in vivo* association of CypB with IRF-3 was only detected 10 min after the infection but not after 30 min. At present, it has been reported that the C-terminal phosphorylation of IRF-3 is mediated by IκB kinase-ε and TANK-binding kinase 1 (10, 11). The mutagenesis of IRF-3 revealed key residues for virus-induced activation. Substitutions of the serine residues at 385 or 386 to alanine, glutamic acid, or aspartic acid made the molecule unresponsive to stimuli (7, 21). Substitutions of other serine/threonine residues, present at positions 396, 398, 402, 404, and 405, to aspartic acid made IRF-3 constitutively active (20). Recently, Servant *et al.* (21) identified Ser-396 and Ser-398 as the minimal phosphorylation sites critical for activation, based on their observation that S396D and S396D/S398D are constitutively active. More recently, Mori *et al.* (23) identified Ser-386 as the target of IRF-3, using an antibody that specifically detects the phosphorylation of Ser-386. As protein kinases are often associated with, in addition to their regulators, molecular chaperones that sometimes need to exert their specificity for the substrates, it is interesting to speculate that CypB associates with the IRF-3 kinases, IκB kinase-ε and TANK-binding kinase 1, in a similar manner. Although it will be important in the future to determine whether it is the CypB binding, catalytic activity, or both that is responsible for its effect on IRF-3, our results indicate that CypB plays a significant role in modulating IFN-β gene expression via its interaction with IRF-3.